Online Monitoring of State of Health for AGM Lead Acid Batteries

by

Yumeng Gao

A thesis submitted to the Graduate Faculty of
Auburn University
in partial fulfillment of the
requirements for the Degree of
Master of Science

Auburn, Alabama
August 1, 2015

Keywords: Battery Monitoring System, AGM, State of Health,
Parameter Identification, Power Prediction, Capacity Estimation

Approved by

Song-Yul Choe, Chair, Professor of Mechanical Engineering
Dan Marghitu, Professor of Mechanical Engineering
John Hung, Professor of Electrical and Computer Engineering

Abstract

Prediction of degradation states like power and capacity fade is the most challenging issue for rechargeable batteries, which is called State of Health (SOH). Power and capacity fade is evaluated by predicting Available Power and estimating Maximum Capacity in a battery at any instant. This thesis proposes online estimation methods for SOH of an Absorbed Glass Mat (AGM) lead acid battery based on a second order Randles' equivalent circuit model (ECM). Since the Maximum Capacity can be simply predicted based on estimated state-of-charge (SOC), this thesis has been mainly focused on prediction of Available Power. The Available Power is calculated based on a maximum allowable current and the terminal voltage using a second order Randles' ECM. However, the parameters of the model vary continuously because of effects of amplitude of current, temperature, SOC in addition to aging process. After review of different methods of parameter estimations, I reformulated the continuous equation of the model into a difference equation of the Autoregressive Model with Exogenous input (ARX) and applied Linear Kalman Filter (LKF) to estimate the parameters. The performance of this technique has been better than recursive least square (RLS) methods, particularly at rapidly varying parameters optimized by selection of appropriate covariance matrices. In addition, the pre-calculated open circuit voltage (OCV) can reduce the number of the parameters that allows for stability of the estimation. For capacity fade, the Maximum Capacity is estimated using RLS under assumption that SOC is known. Experimental validation of both Available Power prediction and Maximum Capacity

estimation are conducted under aging condition as batteries are cycled. At the end, this thesis shows evaluation of SOH using the Available Power and Maximum Capacity.

Acknowledgement

I would like to express my deep appreciation to my advisor, Dr. Song-yul Choe, for giving me the opportunity to get involved in this research project. His wise suggestions and generous guidance assisted me to the fulfillment of my study. Without his valuable suggestions and detailed corrections to my papers and dissertation, I would hardly finish my research program. I also would like to acknowledge to my committee members, Dr. John Hung and Dr. Dan Marghitu, for their continuous instructions and encouragement, which enabled me to develop a deep understanding in the research area. Last but not least, I would like to express my gratitude to my parents, Jiantao Gao and Jing Chen, for their unselfish support of my academic endeavor.

Table of Contents

List of Tables

List of Figures

List of Abbreviations

AGM	Absorbed Glass Mat
ARX	Autoregressive model with exogenous input
BMS	Battery management system
ECM	Equivalent circuit model
EIS	Electrochemical impedance spectroscopy
EMF	Electromotive force
HPPC	Hybrid pulse power characterization
KF	Kalman filter
IBS	Intelligent battery sensor
LKF	Linear Kalman filter
OCV	Open circuit voltage
RLS	Recursive least squares
SOC	State of Charge
SOF	State of Function
SOH	State of Health
UKF	Unscented Kalman filter

List of Symbols

C	Capacitor (F)
E	Electric potential (V)
F	Faraday's constant (96,487 $Coulombs \cdot mol^{-1}$)
G	Gibbs free energy
H	Enthalpy ($J \cdot kg^{-1}$)
I	Current (A)
K	Update gain
OCV	Open circuit voltage (V)
P	Power (W) or error covariance matrix
Q	Reaction quotient or process covariance matrix
Q_{max}	Maximum Capacity of a battery at present aging condition
R	Resistance (Ω), universal gas constant (8.314 $J \cdot mol^{-1} \cdot K^{-1}$) , or measurement covariance matrix
S	Entropy ($J \cdot K^{-1} \cdot kg^{-1}$)
T	Absolute temperature (K)
V_t	Terminal voltage of a battery (V)
W	Weighting factor matrix

Greek symbols

η	Over-potential (V)

θ	Parameters
φ	Vector of known variables
λ	Forgetting factor

1. Introduction

1.1. Background

As the transportation industry strives to electrify vehicles, the onboard battery management system (BMS) becomes one of the major issues that need further development. BMS monitors various states of a battery, such as current, voltage, temperature, State of Charge (SOC), and State of Health (SOH) [1]. Successfully monitoring of these states can prevent a battery from various damages, and they can also significantly improve the battery performance in a vehicle. This thesis focus on the algorithm development of SOH, including Available Power Prediction and Capacity Estimation.

The major batteries used in a traditional vehicle are Lead acid batteries due to its low cost and safety consideration. Absorbed Glass Mat (AGM) battery became popular in early 1980s. It is capable to deliver a higher power on demand and offers a relatively longer service life than other types of Lead acid batteries. Thus, it is commonly used in a high-end vehicle that includes lots of power-hungry accessories, such as heated steering wheels, heated seats, and heated mirrors. AGM batteries were used to conduct required experiments in this thesis.

1.1.1. Basics of AGM Batteries

AGM is an improved technology of Lead acid battery, and it can have a better performance than a regular flooded type Lead acid battery. The major difference in structure is that there is a mat of fine glass fibers that absorbed the electrolyte in an AGM battery. Obviously, this difference makes the AGM battery spill free, so that the hazardous material inside won't spill out easily. Secondly, this improvement also reduces its internal resistance as compared with the regular type. A lower internal resistance allows a higher current output, thus the maximum Available Power of the battery is increased. Other advantages over regular flooded type Lead acid batteries are longer service life, lower weight, faster charge time, and better electrical reliability. On the other hand, there are a few disadvantages of AGM batteries. It has a lower specific energy and higher manufacturing costs.

Figure 1: A typical AGM battery in high-end vehicles

1.1.2. Fundamental Chemical Reactions in AGM batteries

There are plenty of chemical reactions in a Lead acid battery. Paul [2] has made a fully discussion about the chemical reactions at different potential-pH. The major reaction in a Lead acid battery is:

$$Pb + PbO_2 + 2H_2SO_4 \underset{\text{charging}}{\overset{\text{discharging}}{\rightleftharpoons}} 2PbSO_4 + 2H_2O \quad (1)$$

In discharging, lead and lead dioxide dissolve into the electrolyte forming $PbSO_4$ and water. The chemical energy is converted to electrical energy in this reaction while this process is reversed in charging condition.

In thermodynamics, the Gibbs free energy is defined as:

$$G = H - TS \quad (2)$$

, where H is enthalpy, T is absolute temperature, and S is entropy

In chemical reaction, the variation of the equation (2) is used:

$$\Delta G = \Delta H - T\Delta S \quad (3)$$

Thus, change of the free energy during chemical reaction is expressed as:

$$\Delta G = \Delta G^0 - RT \ln Q \quad (4)$$

, where ΔG^0 is the change of standard Gibbs'free energy, R is the ideal gas constant, and Q is the reaction quotient

The potential of electrode in standard state condition is:

$$E = -\frac{\Delta G}{n \cdot F} \quad (5)$$

, where n is the number of electrons involved in the redox reaction, F is the Faraday's constant

Combining (4) and (5), the redox potential of an electrode is defined by Nernst expression:

$$E = E^0 + \frac{RT}{nF}\ln Q \quad (6)$$

, where E^0 is the potential of electrode under standard conditions

The overall Electromotive force (EMF) is defined as:

$$E = E^0_{Cathode} - E^0_{Anode} - \eta \quad (7)$$

, where η is over-potential

The major chemical reaction at positive electrode and its potential under standard condition is:

$$Pb + H_2SO_4 \underset{\text{charging}}{\overset{\text{discharging}}{\rightleftharpoons}} PbSO_4 + 2H^+ + 2e^-;\ E^0_{Anode} = -0.356V \quad (8)$$

The major chemical reaction at negative electrode and its potential under standard condition is:

$$PbO_2 + H_2SO_4 + 2H^+ + 2e^- \underset{\text{charging}}{\overset{\text{discharging}}{\rightleftharpoons}} PbSO_4 + 2H_2O;\ E^0_{Cathode} = 1.685V \quad (9)$$

(8) and (9) can be combined into one overall reaction and its potential under standard condition is:

$$Pb + PbO_2 + 2H_2SO_4 \underset{\text{charging}}{\overset{\text{discharging}}{\rightleftharpoons}} 2PbSO_4 + 2H_2O;\ E^0_{Overall} = 2.041V \quad (10)$$

Besides, there are also some side reactions that take place in Lead acid batteries. The major side reaction at positive electrode and negative electrode are as follows:

$$Pb + H_2SO_4 \rightarrow PbSO_4 + 2H^+ + 2e^-;\ E_0 = -0.358V \quad (11)$$

$$2Pb + SO_4^{2-} + H_2O \rightarrow PbO \cdot PbSO_4 + 2H^+ + 4e^-;\ E_0 = -0.130V \quad (12)$$

1.1.3. Intelligent Battery Sensor (IBS)

Intelligent Battery Sensor (IBS) is a mechatronic component that used for online monitoring the battery conditions in a vehicle. It is connected to the negative terminal of the AGM lead acid battery. The IBS is shown in Figure 2.

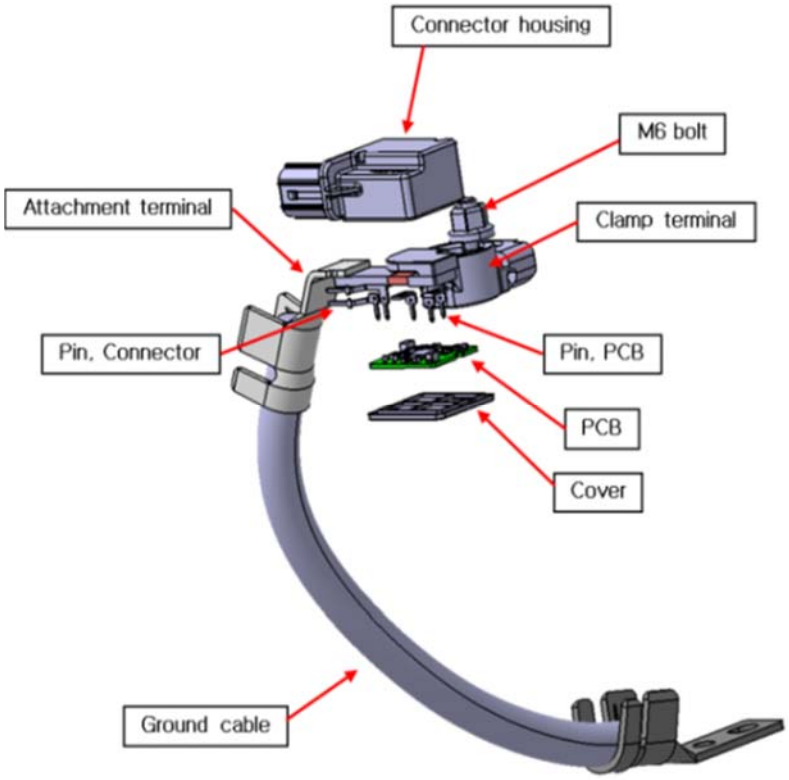

Figure 2: The structure of a typical IBS

The software in the PC-board of the IBS can calculate SOC and SOH of the battery based on the measurement data including current, terminal voltage and temperature. Typical configuration of SLI system with IBS is shown in Figure 3.

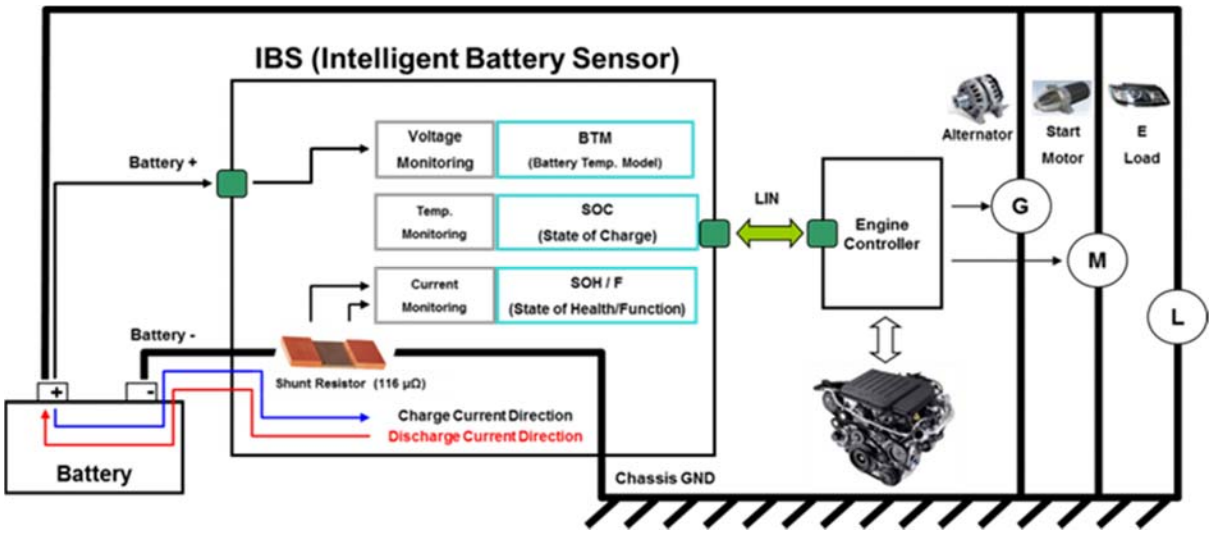

Figure 3: Configuration of SLI system

1.2. Motivations and Objectives

The main objectives of BMS are protecting a battery from damage, prolonging the lifetime of a battery, and maintaining the battery in a required state. It is one of the key components in a vehicle. As there are more and more electrical activities in vehicles, researchers give more and more focus on BMS. Most researchers, e.g. [3] [4] [5] [6] [7, 7] [8] [9] [10] [11] [12], discussed BMS based on lithium-ion batteries., while only a few, e.g. [13] [14] [15] [16], focused on lead acid batteries. Lead acid batteries are still widely used in vehicles, and need to conduct more research on this area. Researchers, e.g. Waag [17] and [18], have done an in-depth review of current BMS technologies for lithium-ion batteries. Most of these technologies can be applied to Lead-acid batteries as well, but their performances are not as good as lithium-ion batteries. The main reason is the different electrochemistry inside a battery. Those algorithms should be improved to fit for lead acid batteries, and BMS in Lead acid batteries still need further development.

BMS plays an important role of protecting the battery from dangerous conditions. A simple BMS may only monitor the current, voltage, and temperature. These can prevent the problems, including over-current, over-voltage, under-voltage, over-temperature, and under-temperature. However, these functions are not enough for a vehicle that has various power-hungry accessories. It is because batteries may not have enough power to carry out certain electrical activities or may not have enough energy to support an activity for a certain time. In this case, Monitoring SOH becomes a solution.

Monitoring of batteries is a challenging task, because it involves complicated electrochemistry systems and has nonlinear behavior that related to a variety of internal and external conditions. Moreover, there are some significant changes in a battery's characteristics when the battery ages, and this make it rather difficult to predict a battery behavior. Thus, advanced batteries algorithms are needed for BMS.

There are certain criterions of the development of SOH for an AGM battery. One of the major criterions is the computational limitation. These batteries algorithms will be implemented into a microcontroller, which only has limited computational power. Thus, complicated models, such as electrochemical model, is avoided while a simple model, such as equivalent circuit model, is considered. Secondly, there is limited memory space in a microcontroller, Recursive methods are preferred, because they only need to store a few information and the information can update in each sample time. Lastly, the estimation results should have a high accuracy and reliability. Thus, advanced estimation techniques should be applied to achieve the required performance.

There are also some other requirements for BMS in a lead acid battery. One is the terminal voltage limitation of a battery. Generally, the maximum terminal voltage of a lead acid battery is

14.3 V, and the minimum terminal voltage is 10.5V (not including cranking). The reason is that a battery will be damaged when exceeding these voltage limits.

The objectives of this thesis are to develop estimation and monitoring algorithms of AGM batteries. Consistent with the objectives, major topics to be addressed are listed as below:

- Identification of batteries parameters
- Prediction of Available Power
- Estimation of Maximum Capacity

1.3. Thesis Outlines

The basic structure of the thesis is shown as follows:

1. Introduction

   First of all, this chapter discusses the research background. It also briefly introduces the basics of AGM batteries and the fundamental chemical reactions of a Lead acid battery. Then, the motivations and objectives of this thesis are addressed.

2. Available Power Prediction

   This Chapter is the main focus in this thesis. First of all, this section introduces the Modeling of AGM batteries. After reviewing the various modeling methods, we selected Randles' ECM to simulate the voltage response of AGM batteries. A fitting comparison is used to compare the fitting performance of different order of Randles' ECM. This thesis shows the continuous equations of those models as well as the conversion process from continuous to discrete equations. Then, Parameters Identification methods are discussed. Two online parameters identification methods are proposed. Through simulation, I compare them and select a better approach. Then, this approach is validated both in simulation and experimental

data. Lastly, this section shows the Power Prediction process with those estimated parameters. This section shows three approaches to predict Available Power of a battery. One approach is selected and the experimental validation of that is shown in the aged process.

3. Maximum Capacity Estimation

In this chapter, the methods for estimation of Maximum Capacity are discussed. RLS is chose to be the final solution. Experimental validation capacity fade is shown in aging condition.

4. Evaluation of SOH

In this section, this thesis discusses how to make use of Available Power and capacity information to evaluate the SOH, and how to detect the battery failures.

5. Conclusion and Future Research

I summarize the main findings in this thesis and discuss the remaining works to do in the future.

2. Available Power Prediction

2.1. Overview

Available Power is the capability of batteries to deliver a certain power at any instant in the course of lifespan. Some researchers [19] also defined it as State of Function (SOF). The Available Power of a battery is the maximum charging and discharging power available under different SOCs, temperatures, and aging process. During aging process, the Available Power gradually decreases, which is referred as Power fade or SOH_P. Prediction of Available Power plays an important role in vehicles. If the battery cannot deliver a certain amount of power for acceleration of actuators like the starter, engine cannot be cranked. If the charging current is too high, the terminal voltage of the battery becomes too high and as a result the battery is overcharged and the lifetime gets reduced. Reduction of the lifetime can be prevented if Available Power can be predicted and considered before the charging.

Existing techniques for prediction of Available Power can be divided into two categories, based on characteristic map or a model.

In the first category, authors [20] [21] recorded all experimental data in a characteristic map that is used to predict Available Power. It is very simple and can be easily implemented. However, this approach only considers the static power and has a low accuracy, because batteries' characteristics are strongly depend on previous load history even in the same SOC, temperature and aging conditions. In addition, this approach does not work well for aging batteries, since the current aging condition is hard to define.

The second one is based on a battery model. Static power can be predicted by using the limiting terminal voltage. However, dynamic power can be predicted by the maximum current allowed over certain period of time through iteratively calculating the battery's terminal voltage response until it reaches to the limiting values. Then, the Available Power is obtained by multiplying the maximum current with the terminal voltage. This technique can significantly increase the estimation accuracy, which can be found in [1] [22] [19] [23] [4] [24] [9]. Main differences in their research are type of model used for parameters identification. The models are based on ECM with either the first order or second order or state space representation or ARX. The methods for parameter identifications include EKF, UKF and RLS, where it is assumed that SOC is unknown. With unknown SOC, parameters estimation can work well under assumption that parameters do change slowly. All of methods above proposed have been applied to lithium ion battery, but not to lead acid batteries where parameters are changing rapidly. Therefore, I selected the dynamic power prediction using a second order ECM in ARX form with known SOC and LKF. .

2.2. Modeling of AGM batteries

2.2.1. Review of Modeling Methods

The parameters of a battery are mainly referred to as the impedance parameters. The value of the parameters continuously change along with the present battery conditions, such as SOC, temperature, and aging condition. The parameters have a strong relation with the SOH of a battery and can be directly used to predict the Available Power [24]. Some authors may also use the parameters to estimate the Maximum Capacity of a battery. Thus, batteries' parameters should be identified prior to the development of the SOH algorithms.

The techniques of identifying those parameters can be categorized into three groups.

- Electrochemical Impedance Spectroscopy (EIS).
- Electrochemical Thermal Model (ETM).
- Equivalent Circuit Model (ECM).

The first technique is the most common method to investigate impedance in laboratories. Some researchers, such as [25], have measured the impedance by actively generating specific currents. This method needs extra excitation over a low to high frequency and has not found practical implementation yet. Other authors, such as [26], have developed a passive method, where the current fluctuations are used. However, it requires that current fluctuations must be both significant and periodic in a certain frequency range. These current fluctuations are not commonly present in vehicles, and thus the implementation is very limited.

The second technique considers electrochemical models. There are mainly four approaches related to this group. The first approach [27] utilizes Sigma Point Kalman Filter to estimate electrolyte conductivity based on a single particle model. Then, it finds a relationship between change in electrolyte conductivity and battery resistance. The second approach [28] is also based on a single particle model. It separates the identification process into two parts, the first one that determines the unknown diffusion and boundary control input. The second part applies nonlinear least squares method to identify those unknown parameters. The third approach [29] simplifies the single particle model that depends on cell resistance and solid phase diffusion time of Li^+ species in the positive electrode, and it makes use of online adaptive gradient-based recursive approach to estimate aging parameters. The last approach [30] combines the electrochemical model with a multi-rate particle filter to estimate SOC and parameters simultaneously.

The third technique, Equivalent Circuit Model (ECM), simulates the battery terminal voltage response. Although it may not fully represent the various response of a battery, it significantly reduces the complexity and saves computational power. Approaches can be divided

into three categories. The first category [31] directly uses the nonlinear least squares to estimate parameters based on the nonlinear ECM model. It is very accurate and stable. However, it requires a high demand of memory and computing power, which makes it impractical to apply in a real vehicle. The second category [3] [4] linearizes the nonlinear model into a state space model and various Kalman Filters are applied to estimate states and parameters. The advantages are to estimate the parameters online because the data only needs to be stored in the present time step. The last category [5] [19] converts the state space model into an autoregressive model with exogenous input (ARX). Then, recursive least squares method is applied to identify the battery's parameters, which further simplifies the estimation process and avoids the complicated matrix calculation in the state space model. Batteries parameters identification methods can be summarized into Table 1:

Table 1: Classification of the methods for the estimation of the battery impedance

Approaches for the estimation of the battery parameters	Based on Electrochemical Impedance Spectroscopy	Based on active method [25]
		Based on passive method [26]
	Based on Electrochemical Models	Based on relationship between electrolyte conductivity and battery resistance [27]
		Based on PDE, Pade identifier, and nonlinear least squares method [28]
		Based on adaptive gradient recursive approach [29]

		Based on multi-rate particle filter method [30]
	Based on Equivalent Circuit Models	Based on nonlinear models [31]
		Based on state space models [3] [4]
		Based on Autoregressive models with exogenous input (ARX) [5] [19]

2.2.2. Collection of Measurement Data

Before constructing the models of a battery, the measurement data should be collected. This is because the model is used to simulate the response of certain signals. There are three typical profiles in traditional vehicles, including Constant Current Charging, Constant Voltage Charging, and Constant Current Discharging.

During charging, a battery is first under Constant Current Charging, and then under Constant Voltage Charging. This process is shown in Figure 4:

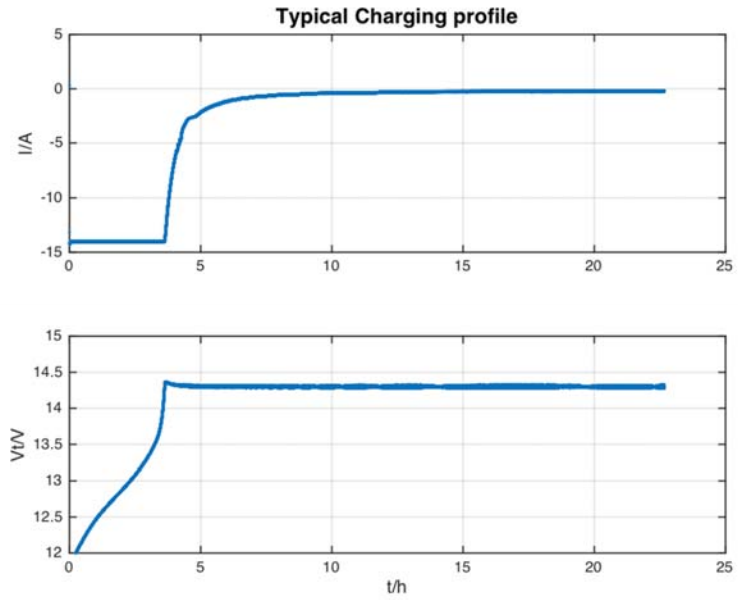

Figure 4: Typical Charging profile

The typical profile during discharging is shown in Figure 5:

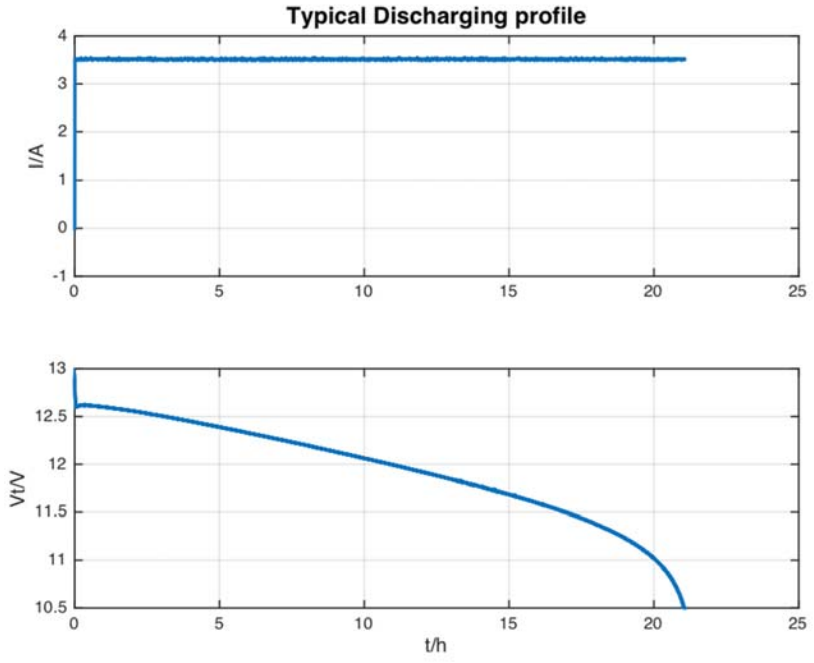

Figure 5: Typical discharging profile

This thesis focuses on Constant Current Charging and Constant Current Discharging because there is no well-developed ECM to simulate the Constant Voltage process in an AGM battery.

2.2.3. Randles' ECM

In this thesis, zeroth order, first order, and second order Randle equivalent circuit models are considered to estimate the parameters of batteries. The advantages and disadvantages of them are discussed. Generally, the lower the model order is, the less time it takes for calculation. On the other hand, the higher the model order is, the more accurate the model's voltage response can represent a real battery. I also use real measured data to compare these three models' voltage responses.

2.2.3.1. The zeroth Order Model

The zeroth order ECM is the simplest and is also referred to as the Ohmic's model. It only consists of two elements, an ideal voltage source and a resistor as shown in Figure 6:

:

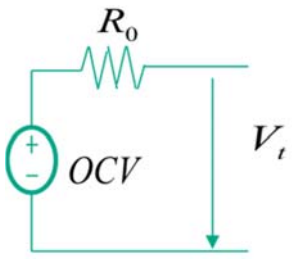

Figure 6: The zeroth order ECM

The voltage source represents the open circuit voltage (OCV) of a battery, and the resistor R_0 represents the internal resistance of a battery. Although the ECM seems to be trivial, it is far

more complicated because the complexity of the parameters it contains. There are only two parameters in this zeroth order ECM, but they are both a function of SOC, temperature, and aging. The parameters also have some relationship with current and time. In order to simplify these parameters, I start from discharging batteries with a constant current at constant temperature and same aging condition. Then, it is can be assumed that the OCV and parameters only depends on SOC. The zeroth order Randles' ECM in continuous time can be derived as follows:

$$V_t = OCV - IR_0 \quad \textbf{(13)}$$

, where the positive sign of the current means discharging.

At 60% SOC, a 3.5A constant discharging current is applied to an AGM battery. The simulated response compared with true response is shown in Figure 7:

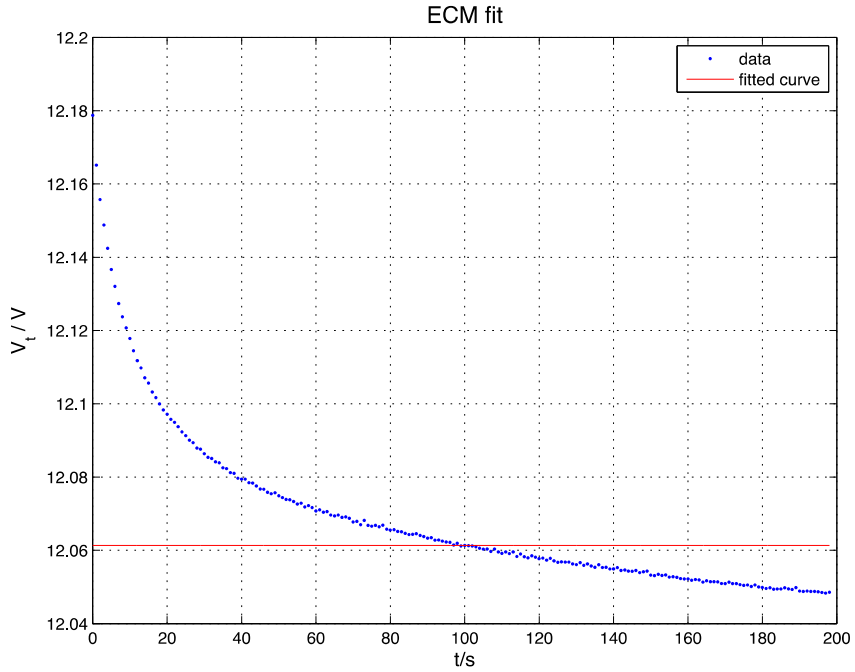

Figure 7: The zeroth order ECM fitting result for a voltage response

As can be seen from Figure 7, the zeroth order ECM has a very poorly fitting performance for the terminal voltage response of a constant current. It fails to capture the dynamics present in

the voltage response of a battery. Actually, the response of a zeroth order ECM is a square wave, and this can represent the immediate voltage drop of a battery. It can be useful for some power applications, because this model is the simplest and has the fewest of parameters to identify.

2.2.3.2. The first Order Model

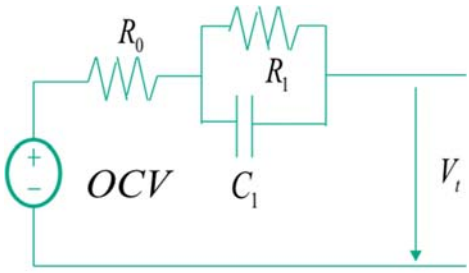

Figure 8: The first order ECM

The first order ECM includes one pair of resistor R_1 and capacitor C_1 in series with the internal resistance R_0. It can represent the terminal voltage response of a constant current better than zeroth order, but it requires two more parameters. The first order ECM is shown in Figure 8:

The added resistor R_1 and capacitor C_1 are functions of SOC, current, temperature, and aging condition. The corresponding equations of this first order ECM become much more complicated. Its inner dynamics in discharging can be represented in following two equations:

$$V_t = OCV - IR_0 - V_{C_1}$$
$$C_1 \frac{dV_{C_1}}{dt} + \frac{V_{C_1}}{R_1} = I \quad V_{C_1}(0) = 0 \qquad (14)$$

In Laplace domain, the second equation in (14) is shown as follows:

$$R_1 C_1 V_{C_1}[s]s + V_{C_1}[s] = IR_1 \frac{1}{s}$$
$$\Rightarrow V_{C_1}[s] = \frac{IR_1}{s(1 + R_1 C_1 s)} = \frac{IR_1 \frac{1}{R_1 C_1}}{s\left(\frac{1}{R_1 C_1} + s\right)} \qquad (15)$$

Then, the result is:

$$V_{C_1} = IR_1\left(1 - e^{-\frac{1}{R_1C_1}t}\right) \quad \textbf{(16)}$$

Combine (16) into the first equation in (14) :

$$V_t = OCV - IR_0 - IR_1\left(1 - e^{-\frac{1}{R_1C_1}t}\right) \quad \textbf{(17)}$$

At 60% SOC, a 3.5A constant discharging current is applied to an AGM battery. The simulated response compared with true response is shown in the Figure 9:

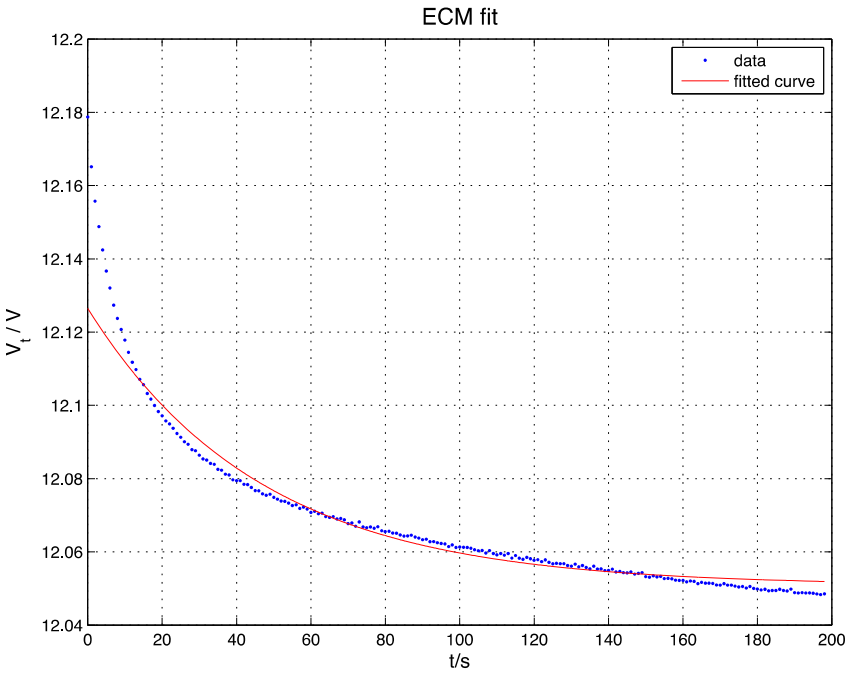

Figure 9: The first order ECM fitting result for a voltage response

In the Figure 9 above, the simulated response is much better than the response of the zeroth order ECM. It can represent the true battery terminal voltage response more accurate, but there are

still some discrepancy, especially in the first 20 seconds. The discrepancy in the beginning stage can lead to a much greater estimation of internal resistance R_0, because the estimated model considering a greater voltage drop as compared with the true battery model. Moreover, the first order ECM requires more computational power than a simple zeroth order ECM, since there are four parameters that need to be identified.

2.2.3.3. The second Order Model

The second order ECM looks very similar to the first order ECM. They both have resistor and capacitor pair, but the difference is that one more pair of resistor and capacitor. The circuit diagram of the second order ECM is shown in the Figure 10:

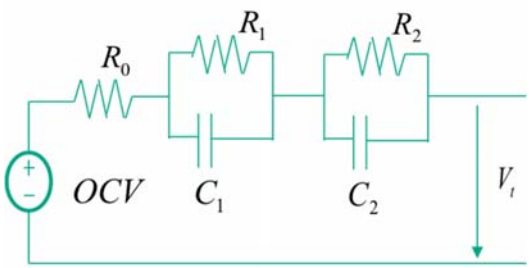

Figure 10: The second order ECM

The total number of the parameters to be estimated is six. The corresponding equations for the second order ECM is shown below:

$$V_t = OCV - IR_0 - V_{C_1} - V_{C_2}$$

$$C_1 \frac{dV_{C_1}}{dt} + \frac{V_{C_1}}{R_1} = I \quad V_{C_1}(0) = 0 \qquad \textbf{(18)}$$

$$C_2 \frac{dV_{C_2}}{dt} + \frac{V_{C_2}}{R_2} = I \quad V_{C_2}(0) = 0$$

Similarly to (15),

$$R_2C_2V_{C_2}s + V_{C_2} = IR_2\frac{1}{s}$$

$$\Rightarrow V_{C_2} = \frac{IR_2}{s(1+R_2C_2s)} = \frac{IR_2\dfrac{1}{R_2C_2}}{s\left(\dfrac{1}{R_2C_2}+s\right)} \qquad \textbf{(19)}$$

Thus,

$$V_{C_2} = IR_2\left(1-e^{-\frac{1}{R_2C_2}t}\right)$$

$$V_t = OCV - IR_0 - IR_1\left(1-e^{-\frac{1}{R_1C_1}t}\right) - IR_2\left(1-e^{-\frac{1}{R_2C_2}t}\right) \qquad \textbf{(20)}$$

At 60% SOC, a 3.5A constant discharging current is applied to an AGM battery. The simulated response compared with true response is shown in Figure 11:

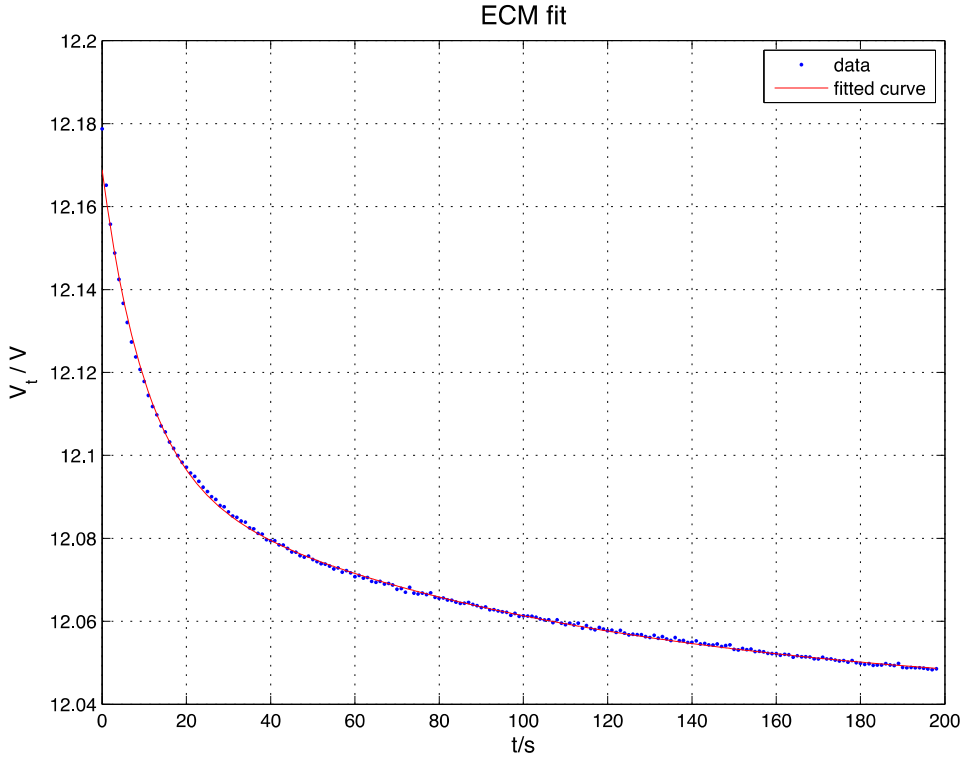

Figure 11: The second order ECM fitting result for a voltage response

As can be seen from Figure 11, the simulated response can trace the terminal voltage response almost perfectly. It can accurately represent the inner dynamics of the terminal voltage response of a battery. However, the second order ECM requires two more parameters to be identified, which cost more computing time and power than the first order ECM.

Comparing these three equivalent circuit models, each Randles' ECM has its advantages and disadvantages. Selecting the best ECM should depend on its applications. In this thesis, the zeroth order ECM is not used because it completely fails to represent the dynamics of an AGM battery. Conversely, both the first order ECM and the second order ECM are considered for parameters identification. I discuss these two models in details at later chapter.

2.3. Online Parameters Identification

2.3.1. Reformulation of Continuous Model

2.3.1.1. OCV Consideration

Before determining these parameters (R_0, R_1, R_2, C_1, C_2), the described models in previous section include one more unknown variable, which is the open circuit voltage (OCV). OCV is the terminal voltage of a battery when the battery is not in charging or discharging conditions. Since the OCV cannot be measured directly, it should be taken into consideration.

There are three approaches. One is estimating the OCV and parameters simultaneously. This method usually makes use of the autoregressive model with exogenous input model. It treats OCV as a parameter and estimate it directly. However, this kind of approach may not be stable enough and may even lead to a divergent result.

The second method is converting OCV to SOC, and then estimating the SOC and parameters simultaneously. SOC is defined as the available capacity divided by the nominal capacity, which is the maximum amount of energy that can be charged into a battery without damaging the battery. The units of SOC are percentage. 100% SOC means the battery is fully charged while 0% indicates the battery is out of energy. Conversion of the OCV to SOC can utilize the OCV-SOC relationship. It is a certain relationship between SOC and OCV. In AGM battery, this relationship remains a relatively a constant value until the battery ages. Thus, it is easy to calculate one value from the other if this relationship is pre-measured. The OCV-SOC curve of the Lead acid batteries used for experiments is shown in Figure 12

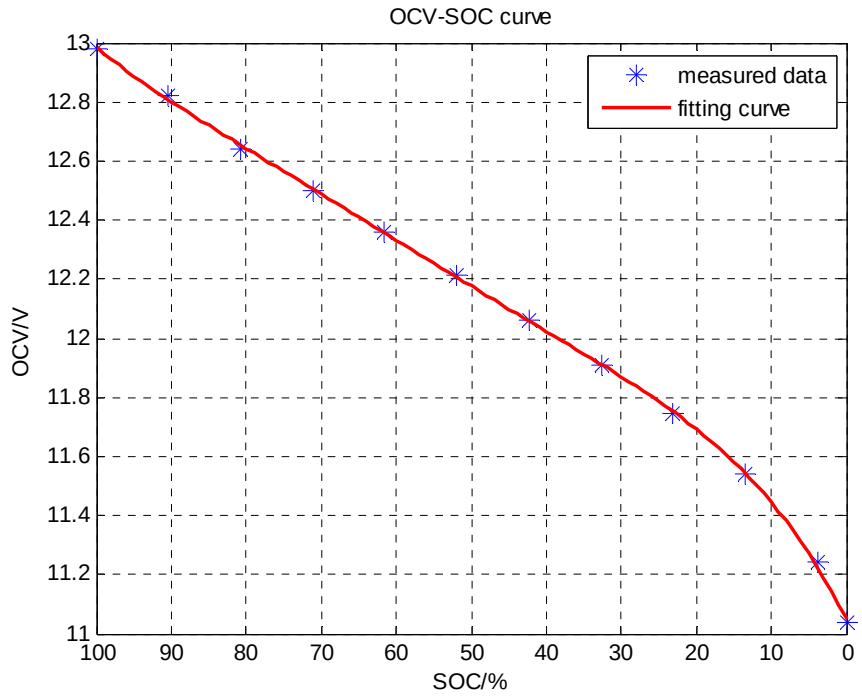

Figure 12: OCV-SOC curve at 25 degree Celsius

OCV-SOC curve for an AGM battery is usually represented by a polynomial. In this thesis, the relationship is defined as follows:

OCV(x) = p1*x^5 + p2*x^4 + p3*x^3 + p4*x^2 + p5*x + p6

Where x is SOC

Parameter	p1	p2	p3	p4	p5	p6
Value	7.134	-21.21	24.36	-13.44	5.086	11.05

On the other hand, the SOC_{k+1} can be expressed based on the SOC_k with the capacity charged or discharged from k to k+1 step.

$$SOC_{k+1} - SOC_k = -\frac{\int_k^{k+1} Idt}{3600 Q_{\max}} \quad \textbf{(21)}$$

, where SOC_k is the SOC at a current sample point and SOC_{k+1} is the SOC at a next sample point, Q_{max} is the estimated Maximum Capacity, and I is the current.

This equation **(21**) of SOC allow a stable result for SOC. It has widely used in the Li-ion batteries, but this co-estimation of SOC and parameters may not have a good performance in Lead acid batteries. It can be used in co-estimation of SOC, but not for parameters. It is because the parameters (R_1, R_2, C_1, C_2) in Lead acid batteries may change with charging time [32], which causes the parameters identification process fluctuating and may even lead to a divergent result. The last approach has three steps:

1. Estimate the SOC by Coulomb Counting
2. Convert the SOC to OCV through the OCV-SOC relationship
3. Treat OCV is a known variable and estimate the parameters with known OCV

Coulomb Counting estimates SOC based on the equation **(21**). This method highly depends on the accuracy of current measurement. Then, the second step is same in the second method,

which is also very reliable. Thus, it can reduce one unknown variable during estimation process in step 3. It makes the estimation process faster and more stable. I propose using the third approach.

2.3.1.2. Continuous Models Representation

The equations of ECM shown in the previous section are all in continuous time. If it is assumed that the current is a constant value, then a nonlinear Least Square method can be directly applied to identify these parameters.

For a first order ECM,

$$V_t = OCV - IR_0 - IR_1\left(1 - e^{-\frac{1}{R_1C_1}t}\right) \Rightarrow OCV - V_t = IR_0 + IR_1\left(1 - e^{-\frac{t}{R_1C_1}}\right) \quad \textbf{(22)}$$

Since OCV can be considered as a known variable (see 2.4.1.1), let $y = OCV - V_t$

$$\begin{aligned} & y = OCV - V_t \\ & \Rightarrow y = IR_0 + IR_1\left(1 - e^{-\frac{t}{R_1C_1}}\right) \\ & \Rightarrow y = \left(R_0 + R_1\right)I - R_1Ie^{-\frac{1}{R_1C_1}t} \end{aligned} \quad \textbf{(23)}$$

Let $a_0 = \left(R_0 + R_1\right)I \quad a_1 = R_1I \quad b = -\dfrac{1}{R_1C_1}$, then $a_0, a_1,$ and b are used to simplify this model:

$$y = a_0 + a_1e^{bt} \quad \textbf{(24)}$$

The simplified model can be identified by nonlinear Least Square method. Matlab function "fit" is used to calculate $a_0, a_1,$ and b. Since I is assumed to be a constant, the parameters are shown as follows:

$$R_1 = -\frac{a_1}{I} \quad R_0 = \frac{a_0}{I} - R_1 \quad C_1 = -\frac{1}{R_1 b} \tag{25}$$

Similarly to first order ECM, the parameters in a second order ECM can be identified:

$$V_t = OCV - IR_0 - IR_1\left(1 - e^{-\frac{1}{R_1C_1}t}\right) - IR_2\left(1 - e^{-\frac{1}{R_2C_2}t}\right) \tag{26}$$

$$\begin{aligned} & y = OCV - V_t \\ & \Rightarrow y = IR_0 + IR_1\left(1 - e^{-\frac{t}{R_1C_1}}\right) - IR_2\left(1 - e^{-\frac{1}{R_2C_2}t}\right) \\ & \Rightarrow y = \left(R_0 + R_1\right)I - R_1Ie^{-\frac{1}{R_1C_1}t} - R_2Ie^{-\frac{1}{R_2C_2}t} \end{aligned} \tag{27}$$

Let $a_0 = \left(R_0 + R_1\right)I \quad a_1 = R_1I \quad a_2 = R_2I \quad b_1 = -\frac{1}{R_1C_1} \quad b_2 = -\frac{1}{R_2C_2}$

$$y = a_0 + a_1e^{b_1t} + a_2e^{b_2t} \tag{28}$$

The parameters can be identified through the following equations:

$$R_1 = -\frac{a_1}{I} \quad R_2 = -\frac{a_2}{I} \quad R_0 = \frac{a_0}{I} - R_1 - R_2 \quad C_1 = -\frac{1}{R_1b_1} \quad C_2 = -\frac{1}{R_2b_2} \tag{29}$$

Although parameters can be identified directly in the continuous time, this approach cannot be used for online parameters identification. One reason is that the current is assumed to be a constant, but the current in real application changes frequently. The other reason is that this nonlinear Least Square fitting process takes relatively more time and consume more memory as compared with discrete model. It needs to store all the prior information, because the fitting process considers all the past data to generate a best fitting curve. If applied online, it needs to run the calculation process in each time step and make it take longer time than recursive Least Square method.

2.3.2. Discretization

In order to identify these parameters online, it is required to convert these continuous models in discrete time. There are two approaches to transfer the continuous model into a discrete model. One is in time domain and the other is to find equation in Laplace domain and then convert them into difference equations. I compare these two transformations and select a better one. All these analysis is discussed based on first order system, because it is easier to calculate and the transformation performance should be the same for both first order and second order ECM.

2.3.2.1. By First Order Taylor Approximation:

For a first order Randles' ECM

$$V_t = OCV - IR_0 - V_{C_1}$$
$$C_1 \frac{dV_{C_1}}{dt} + \frac{V_{C_1}}{R_1} = I \quad \textbf{(30)}$$

$$\frac{dV_{C_1}}{dt} + \frac{V_{C_1}}{R_1 C_1} = \frac{I}{C_1}$$
$$\Rightarrow \frac{V_{C_1}[k+1] - V_{C_1}[k]}{\Delta T} + \frac{V_{C_1}[k]}{R_1 C_1} = \frac{1}{C_1} I[k]$$
$$\Rightarrow V_{C_1}[k+1] = \left(1 - \frac{\Delta T}{R_1 C_1}\right) V_{C_1}[k] + \frac{\Delta T}{C_1} I[k] \quad \textbf{(31)}$$

Let $y[k] = OCV[k] - V_t[k]$,

$$y[k] = OCV[k] - V_t[k]$$
$$\Rightarrow y[k] = R_0 I[k] + V_{C_1}[k] \quad \textbf{(32)}$$

The equation (32) in k-1 time step as:

$$y[k-1] = R_0 I[k-1] + V_{C_1}[k-1]$$
$$\Rightarrow \left(1 - \frac{\Delta T}{R_1 C_1}\right) y[k-1] = \left(1 - \frac{\Delta T}{R_1 C_1}\right) R_0 I[k-1] + \left(1 - \frac{\Delta T}{R_1 C_1}\right) V_{C_1}[k-1] \quad \textbf{(33)}$$

Then, use the equation in present time step (32) to minus the equation in previous time step (33):

$$y[k] - \left(1 - \frac{\Delta T}{R_1 C_1}\right) y[k-1] = R_0 I[k] + V_{C_1}[k] - \left(1 - \frac{\Delta T}{R_1 C_1}\right) R_0 I[k-1] - \left(1 - \frac{\Delta T}{R_1 C_1}\right) V_{C_1}[k-1]$$
$$\Rightarrow y[k] = \left(1 - \frac{\Delta T}{R_1 C_1}\right) y[k-1] + R_0 I[k] - \left(1 - \frac{\Delta T}{R_1 C_1}\right) R_0 I[k-1] + \frac{\Delta T}{C_1} I[k-1] \quad \textbf{(34)}$$

In difference equation form:

$$y[k] = a_1 y[k-1] + b_0 I[k] + b_1 I[k-1] \quad \textbf{(35)}$$

, where $a = \left(1 - \frac{\Delta T}{R_1 C_1}\right), b_0 = R_0, b_1 = \frac{\Delta T}{C_1} - R_0 \left(1 - \frac{\Delta T}{R_1 C_1}\right)$

The parameters can be identified:

$$R_0 = b_0 \quad C_1 = \frac{\Delta T}{b_1 + a_1 b_0} \quad R_1 = \frac{\Delta T}{C_1 (1 - a_1)} \quad \textbf{(36)}$$

2.3.2.2. By Laplace Transform:

$$V_t = OCV - IR_0 - V_{C_1}$$
$$C_1 \frac{dV_{C_1}}{dt} + \frac{V_{C_1}}{R_1} = I \Rightarrow V_{C_1}[s] = \frac{I[s] R_1}{s(1 + R_1 C_1 s)} \quad \textbf{(37)}$$

Combine these two equations in (37):

$$\frac{\mathrm{OCV}[s]-V_t[s]}{s} = \frac{R_0 I[s]}{s} + \frac{R_1 I[s]}{s(1+R_1C_1 s)}$$

$$y[s] = I[s]\frac{R_0R_1C_1 s + R_0 + R_1}{R_1C_1 s + 1} \qquad \textbf{(38)}$$

By using bilinear transformation $s = \frac{2}{\Delta T}\frac{1-z^{-1}}{1+z^{-1}}$,

$$\frac{Y[z^{-1}]}{U[z^{-1}]} = \frac{R_0R_1C_1\left(\frac{2}{\Delta T}\frac{1-z^{-1}}{1+z^{-1}}\right) + R_0 + R_1}{R_1C_1\left(\frac{2}{\Delta T}\frac{1-z^{-1}}{1+z^{-1}}\right) + 1}$$

$$\frac{Y[z^{-1}]}{U[z^{-1}]} = \frac{\frac{R_0\Delta T + R_1\Delta T + 2R_0R_1C_1}{\Delta T + 2R_1C_1} + \frac{R_0\Delta T + R_1\Delta T - 2R_0R_1C_1}{\Delta T + 2R_1C_1}z^{-1}}{1 + \frac{\Delta T - 2R_1C_1}{\Delta T + 2R_1C_1}z^{-1}} \qquad \textbf{(39)}$$

Then, the equation (39) is shown in difference equation form:

$$y[k] = a_1 y[k-1] + b_0 I[k] + b_1 I[k-1] \qquad \textbf{(40)}$$

, where $a_1 = -\frac{\Delta T - 2R_1C_1}{\Delta T + 2R_1C_1}, b_0 = \frac{R_0\Delta T + R_1\Delta T + 2R_0R_1C_1}{\Delta T + 2R_1C_1}, b_1 = \frac{R_0\Delta T + R_1\Delta T - 2R_0R_1C_1}{\Delta T + 2R_1C_1}$

The parameters can be identified:

$$R_0 = \frac{b_0 - b_1}{1+a_1}, R_1 = \frac{b_0 + b_1}{1-a_1} - R_0, C_1 = \frac{\Delta T(1+a_1)}{2(1-a_1)R_1} \qquad \textbf{(41)}$$

2.3.2.3. Comparison of Discretization Methods

The discrete equations derived from time domain and Laplace domain seem to be in the same form. Both contain $a_1, b_0,$ and b_1, which means that they get same values for $a_1, b_0,$ and b_1 in

the parameters identification process. However, the final parameters R_0, R_1, and C_1 are calculated by different equations of $a_1, b_0,$ and b_1.

Suppose that $R_0 = 0.009057\Omega \quad R_1 = 0.0157\Omega \quad C_1 = 2392F$. Matlab are used to simulate response y with a constant input of 14 A. The comparison result is shown in Figure 13:

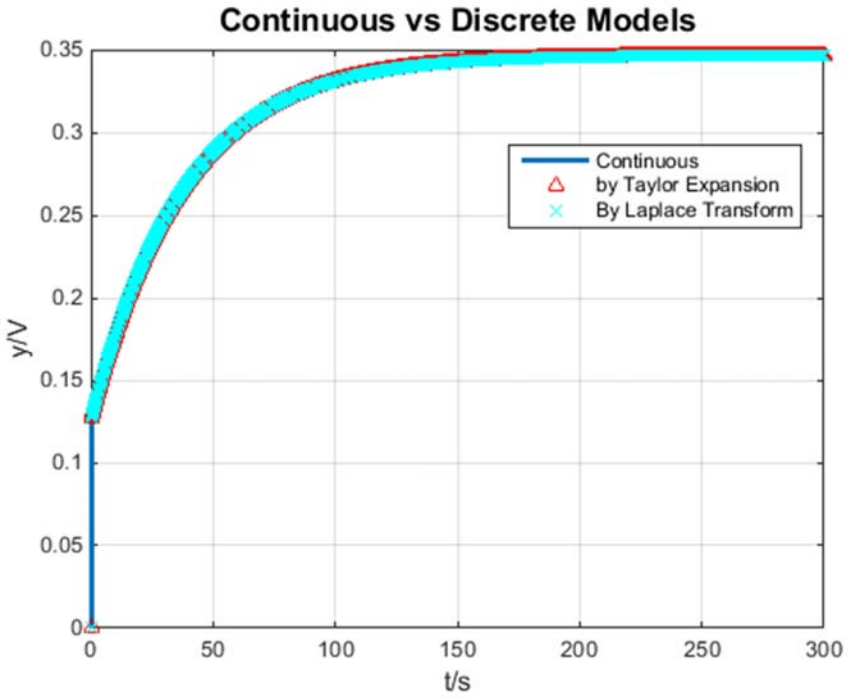

Figure 13: Comparison of continuous and discrete equations

As can be seen in the figure above, both of the two transformation approaches can achieve satisfactory result to simulate the response. However, the equation derived by bilinear transform is much more complicated than the equation derived by Taylor approximation and requires more computational power. Thus, I select the method of Taylor approximation.

2.3.2.4. Final Discrete Model

The second order ECM is selected in the section of Approaches for Parameters Identification in Continuous Model, and time domain is chosen in the Approaches to Convert Continuous Model to Discrete Model. This section shows the final model, which is the Discrete Model of second order ECM in time domain.

For a second order ECM, the continuous models are:

$$V_t = OCV - IR_0 - V_{C_1} - V_{C_2}$$

$$C_1 \frac{dV_{C_1}}{dt} + \frac{V_{C_1}}{R_1} = I \quad V_{C_1}(0) = 0$$

$$C_2 \frac{dV_{C_2}}{dt} + \frac{V_{C_2}}{R_2} = I \quad V_{C_2}(0) = 0 \qquad \textbf{(42)}$$

Through Taylor Expansion, the following two equations can be derived:

$$\frac{dV_{C_1}}{dt} + \frac{V_{C_1}}{R_1C_1} = \frac{I}{C_1} \Rightarrow \frac{V_{C_1}[k+1] - V_{C_1}[k]}{\Delta T} + \frac{V_{C_1}[k]}{R_1C_1} = \frac{1}{C_1} I[k] \Rightarrow V_{C_1}[k+1] = \left(1 - \frac{\Delta T}{R_1C_1}\right) V_{C_1}[k] + \frac{\Delta T}{C_1} I[k]$$

$$\frac{dV_{C_2}}{dt} + \frac{V_{C_2}}{R_2C_2} = \frac{I}{C_2} \Rightarrow \frac{V_{C_2}[k+1] - V_{C_2}[k]}{\Delta T} + \frac{V_{C_2}[k]}{R_2C_2} = \frac{1}{C_2} I[k] \Rightarrow V_{C_2}[k+1] = \left(1 - \frac{\Delta T}{R_2C_2}\right) V_{C_2}[k] + \frac{\Delta T}{C_2} I[k]$$

Let $y[k] = OCV[k] - V_t[k]$,

$$OCV[k] - V_t[k] = R_0 I[k] + V_{C_1}[k] + V_{C_2}[k]$$

$$y[k] = R_0 I[k] + \left(1 - \frac{\Delta T}{R_1C_1}\right) V_{C_1}[k-1] + I[k-1]\frac{\Delta T}{C_1} + V_{C_2}[k] \qquad \textbf{(43)}$$

Let $a_1 = \left(1 - \frac{\Delta T}{R_1C_1}\right)$, the previous time step of (43):

$$a_1 y[k-1] = a_1 R_0 I[k-2] + a_1 V_{C_1}[k-2] + a_1 V_{C_2}[k-1] \qquad \textbf{(44)}$$

Using the equation in current time step minus the last time step:

$$y[k]-a_1y[k-1]=R_0I[k]+[\frac{\Delta T}{C_1}-a_1R_0]I[k-1]+V_{C_2}[k]-a_1V_{C_2}[k-1] \quad \textbf{(45)}$$

In previous time step of **(57)**, let $a_2=\left(1-\frac{\Delta T}{R_2C_2}\right)$:

$$a_2y[k-1]-a_2a_1y[k-2]=a_2R_0I[k-1]+a_2[\frac{\Delta T}{C_1}-a_1R_0]I[k-2]+a_2V_{C_2}[k-1]+a_2a_1V_{C_2}[k-2] \quad \textbf{(46)}$$

Using the equation in last time step minus the second last time step:

$$\begin{aligned}
&y[k]-(a_1+a_2)y[k-1]+a_1a_2y[k-2]\\
&=R_0I[k]+\left[\frac{\Delta T}{C_1}-a_1R_0-a_2R_0\right]I[k-1]-a_2[\frac{\Delta T}{C_1}-a_1R_0]I[k-2]+\frac{\Delta T}{C_2}I[k-1]-a_1\frac{\Delta T}{C_2}I[k-2]\\
&\Rightarrow y[k]=(a_1+a_2)y[k-1]-a_1a_2y[k-2]+R_0I[k]+\left[\frac{\Delta T}{C_1}+\frac{\Delta T}{C_2}-a_1R_0-a_2R_0\right]I[k-1]+[a_1a_2R_0-\frac{\Delta T}{C_1}a_2-\frac{\Delta T}{C_2}a_1]I[k-2]
\end{aligned} \quad \textbf{(47)}$$

Thus, the final model is:

$$y[k]=\theta_1y[k-1]+\theta_2y[k-2]+\theta_3I[k]+\theta_4I[k-1]+\theta_5I[k-2] \quad \textbf{(48)}$$

, where

$$\theta_1=a_1+a_2,\theta_2=a_1a_2,\theta_3=R_0,\theta_4=\frac{T_s}{C_1}+\frac{T_s}{C_2}-R_0\left(a_1+a_2\right),$$

$$\theta_5=R_0a_1a_2-a_2\frac{T_s}{C_1}-a_1\frac{T_s}{C_2},a_1=1-\frac{T_s}{R_1C_1},a_2=1-\frac{T_s}{R_2C_2}$$

The parameters can be identified:

$$a_1=\frac{\theta_1+\sqrt{\theta_1^2+4\theta_2}}{2},a_2=\frac{\theta_1-\sqrt{\theta_1^2+4\theta_2}}{2},R_0=\theta_3,$$

$$C_1=\frac{\Delta T\sqrt{\theta_1^2+4\theta_2}}{a_1(\theta_4+\theta_1\theta_3)+\theta_5+\theta_2\theta_3},C_2=\frac{\Delta T}{\theta_4+\theta_1\theta_3-\frac{\Delta T}{C_1}},R_1=\frac{\Delta T}{C_1(1-a_1)},R_2=\frac{\Delta T}{C_2(1-a_2)}$$

2.3.3. Approaches to Parameters Identification using Discrete Model

2.3.3.1. Recursive Least-square (RLS) Method

This section introduces the method to identify these parameters by recursive Least-squares (RLS) method. It is the most basic way to identify parameters in a system. This section also introduces its improved version, which is called RLS with forgetting factor.

Before introducing the RLS, the Least Squares method is briefly explained because RLS is just a recursive form of Least Square method. Let us consider an Autoregressive model with exogenous input (ARX) system:

$$A(z)y(k) = B(z)u(k) + e(k) \quad (k = \ 1 \quad 2 \quad \cdots \ ) \tag{49}$$

, where $A(z) = 1 + a_1 z^{-1} + \cdots + a_n z^{-n}$, y(k) is the output at k step, $B(z) = b_0 + b_1 z^{-1} + \cdots + b_m z^{-m}$, u(k) is the exogenous input at k step, and e is the disturbance

The ARX model is one of the standard estimation models for Least Squares. In the Least Squares estimation form, it is written as follows:

$$y(k) = \phi^T(k)\hat{\theta} \tag{50}$$

, where $\phi^T(k) = \begin{bmatrix} -y(k-1) & \cdots & -y(k-n) & u(k) & \cdots & u(k-m) \end{bmatrix}$ represents the known variables, and $\hat{\theta} = \begin{bmatrix} \hat{a}_1 & \cdots & \hat{a}_n & \hat{b}_0 & \cdots & \hat{b}_m \end{bmatrix}^T$ represents the parameters need to be identified.

During a time interval $1 \le t \le N$, input and output data collected are as follows:

$$Z^N = \{u(1), y(1), \ldots, u(N), y(N)\} \tag{51}$$

The Least Squares method minimizes the mean square error to estimate the optimum parameters $\hat{\theta}$. The loss function of a common Least Squares is:

$$V\left(\hat{\theta}, Z^N\right) = \frac{1}{N}\sum_{k=1}^{N}\frac{1}{2}\left[y(k) - \phi^T(k)\hat{\theta}\right]^2 \quad \textbf{(52)}$$

In order to get a minimal value with regard to parameters, the loss function is differentiated:

$$\frac{dV\left(\hat{\theta}, Z^N\right)}{d\theta} = -\frac{1}{N}\sum_{k=1}^{N}\left[y(k) - \phi^T(k)\hat{\theta}\right]\phi^T(k) = 0 \quad \textbf{(53)}$$

In matrix form, $y(k) = \phi^T(k)\hat{\theta}$ can be represented as:

$$Y(N) = \Phi(N)\hat{\theta} \quad \textbf{(54)}$$

, where $Y(N) = \begin{bmatrix} y(k_0) \\ y(k_0+1) \\ \vdots \\ y(N) \end{bmatrix}$,

$$\Phi(N) = \begin{bmatrix} \phi^T(k_0) \\ \phi^T(k_0+1) \\ \vdots \\ \phi^T(N) \end{bmatrix} = \begin{bmatrix} -y(k_0-1) & \cdots & -y(k_0-n) & u(k_0) & \cdots & u(k_0-m) \\ -y(k_0) & \cdots & -y(k_0-n+1) & u(k_0+1) & \cdots & u(k_0-m+1) \\ & & \vdots & & & \\ -y(N-1) & \cdots & -y(N-n) & u(N) & \cdots & u(N-m) \end{bmatrix}$$

Assume matrix is nonsingular, and then the parameters can be identified in the following steps:

$$\begin{aligned} &\Phi\hat{\theta} = Y \\ &\Phi^T\Phi\hat{\theta} = \Phi^T Y \\ &\Rightarrow \hat{\theta} = (\Phi^T\Phi)^{-1}\Phi^T Y \end{aligned} \quad \textbf{(55)}$$

When there are some parameters that appear to be abnormal or people want to focus on some important parameters, a weighting factor matrix W can be added to adjust the weight of these parameters during identification process.

$$\hat{\theta} = (\Phi^T W \Phi)^{-1} \Phi^T W Y \quad \textbf{(56)}$$

As can be seen, the Least Squares method estimates the parameters in one single step considering all the measured data. In order to make this process recursive, two extra notations should be introduced:

$$P(k) = [\Phi^T(k)\Phi(k)]^{-1} = [\sum_{i=1}^{k} \phi(i)\phi^T(i)]^{-1} \quad \textbf{(57)}$$
$$K(k) = P(k)\phi(k)$$

For the current step,

$$\hat{\theta} = (\Phi^T\Phi)^{-1}\Phi^T Y \Rightarrow \hat{\theta}(k) = P(k)[\sum_{i=1}^{k} \phi(i)y(i)] = P(k)[\sum_{i=1}^{k-1} \phi(i)y(i) + \phi(k)y(k)] \quad \textbf{(58)}$$

For the last step,

$$\hat{\theta}(k-1) = P(k-1)[\sum_{i=1}^{k-1} \phi(i)y(i)] \Rightarrow \sum_{i=1}^{k-1} \phi(i)y(i) = P^{-1}(k-1)\hat{\theta}(k-1) \quad \textbf{(59)}$$

Then,

$$P^{-1}(k) = \sum_{i=1}^{k} \phi(i)\phi^T(i) = \sum_{i=1}^{k-1} \phi(i)\phi^T(i) + \phi(k)\phi^T(k) = P^{-1}(k-1) + \phi(k)\phi^T(k) \quad \textbf{(60)}$$
$$\Rightarrow P^{-1}(k-1) = P^{-1}(k) - \phi(k)\phi^T(k)$$

Plug the result **(60)** back to the last step equation **(59)**

$$\sum_{i=1}^{k-1} \phi(i)y(i) = \left[P^{-1}(k) - \phi(k)\phi^T(k)\right]\hat{\theta}(k-1) \quad \textbf{(61)}$$

Plug the result **(61)** back to the current step equation **(58)**

$$\hat{\theta}(k) = P(k)\left\langle\left\{\left[P^{-1}(k) - \phi(k)\phi^T(k)\right]\hat{\theta}(k-1)\right\} + \phi(k)y(k)\right\rangle$$
$$\Rightarrow \hat{\theta}(k) = \hat{\theta}(k-1) - P(k)\phi(k)\phi^T(k)\hat{\theta}(k-1) + P(k)\phi(k)y(k) \quad \textbf{(62)}$$
$$\Rightarrow \hat{\theta}(k) = \hat{\theta}(k-1) + K(k)\varepsilon(k)$$

Then P(k) and K(k) are also need to be updated

$$P(k) = [\Phi^T(k)\Phi(k)]^{-1} = \left[\Phi^T(k-1)\Phi(k-1) + \phi(k)\phi^T(k)\right]^{-1}$$
$$= \left[P^{-1}(k-1) + \phi(k)\phi^T(k)\right]^{-1} \quad \textbf{(63)}$$

By matrix inversion lemma: $(A+BCD)^{-1} = A^{-1} - A^{-1}B(C^{-1} + DA^{-1}B)^{-1}DA^{-1}$

$$P(k) = P(k-1) - P(k-1)\phi(k)\left[I + \phi^T(k)P(k-1)\phi(k)\right]^{-1}\phi^T(k)P(k-1) \quad \textbf{(64)}$$

$$K(k) = P(k)\phi(k) = P(k-1)\phi(k)\left\{I - \left[I + \phi^T(k)P(k-1)\phi(k)\right]^{-1}\phi^T(k)P(k-1)\phi(k)\right\}$$
$$\Rightarrow K(k) = P(k-1)\phi(k)[I + \phi^T(k)P(k-1)\phi(k)]^{-1} \quad \textbf{(65)}$$

In summary, an initial condition should be provided at first:

$$P(k_0) = [\Phi^T(k_0)\Phi(k_0)]^{-1} \quad \textbf{(66)}$$
$$\hat{\theta}(k_0) = P(k_0)\Phi^T(k_0)Y(k_0)$$

Then, it is assumed that $\Phi^T\Phi$ is non-singular for all k. Thus, the parameters can be updated in each step as follows:

$$K(k) = \frac{P(k-1)\phi(k)}{I + \phi^T(k)P(k-1)\phi(k)}$$
$$\hat{\theta}(k) = \hat{\theta}(k-1) + K(k)[y(k) - \phi^T(k)\hat{\theta}(k-1)] \quad \textbf{(67)}$$
$$P(k) = P(k-1) - K(k)\phi^T(k)P(k-1)$$

Since the parameters are a function of temperature, SOC, current, and aging, the true parameter values may continuously change during estimation process. Thus, it is better to give a high weight factor on the most recent measurement data. This can be done with a forgetting factor λ that makes the previous data less important. The estimation steps become:

$$K(k) = \frac{P(k-1)\phi(k)}{\lambda + \phi^T(k)P(k-1)\phi(k)}$$
$$\hat{\theta}(k) = \hat{\theta}(k-1) + K(k)[y(k) - \phi^T(k)\hat{\theta}(k-1)] \quad (68)$$
$$P(k) = \frac{P(k-1) - K(k)\phi^T(k)P(k-1)}{\lambda}$$

2.3.3.2. Kalman Filter (KF) Method

KF can also be used for parameters identification in ARX model. Firstly, the standard KF method is briefly discussed. Consider a state space model with noises, w_k and v_k:

$$\mathbf{x}_k = \varphi_k \mathbf{x}_{k-1} + B_k u_{k-1} + w_{k-1} \quad (69)$$
$$\mathbf{z}_k = H_k \mathbf{x}_k + v_k$$

$$E(w_k w_i^T) = Q_k, \quad i = k$$
$$0, \quad i \neq k$$

, where the covariance of this model are: $E(v_k v_i^T) = R_k, \quad i = k$

$$0, \quad i \neq k$$
$$E(w_k v_i^T) = 0, \quad \text{for all k and i}$$

The state update of this algorithm is:

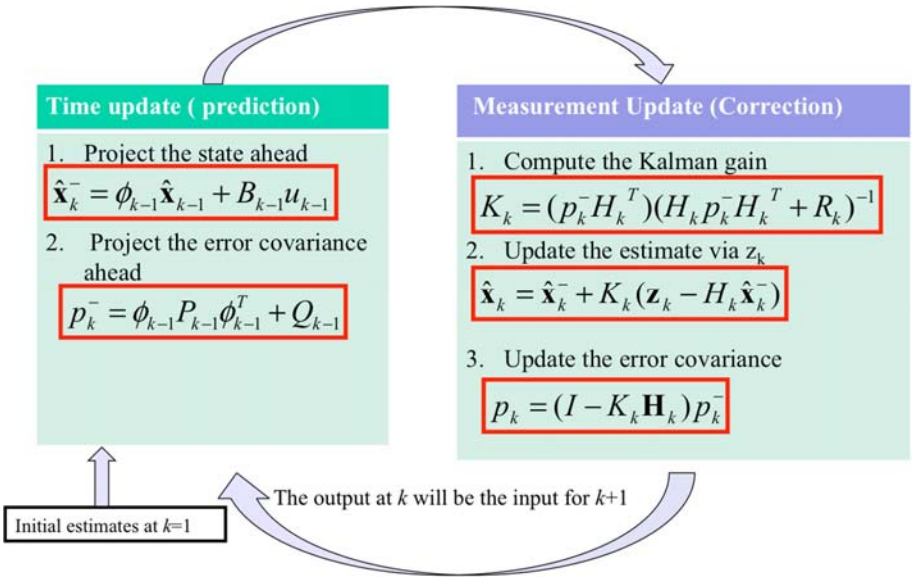

Figure 14: Standard Kalman Filter process

Under consideration that the parameters are states, the Kalman Filter can be directly applied to the ARX model:

$$\begin{aligned}\mathbf{x}_k &= \phi_k \cdot \mathbf{x}_{k-1} + w_{k-1} \\ \mathbf{z}_k &= H \cdot \mathbf{x}_k + v_k\end{aligned} \quad \xrightarrow[z = y \quad H = \varphi^T]{x = \theta \quad \phi = I} \quad \begin{aligned}\theta(k) &= \theta(k-1) + \omega(k-1) \\ y(k) &= \varphi^T(k)\theta(k) + v(k)\end{aligned}$$

Then, the parameters identification process becomes:

$$\begin{aligned}K(k) &= \frac{P(k-1)\phi(k)}{R + \phi^T(k)P(k-1)\phi(k)} \\ \hat{\theta}(k) &= \hat{\theta}(k-1) + K(k)[y(k) - \phi^T(k)\hat{\theta}(k-1)] \\ P(k) &= P(k-1) - K(k)\phi^T(k)P(k-1) + Q\end{aligned} \qquad \textbf{(70)}$$

When I compare RLS with LKF, performance of them is quite similar. The major difference is the update of error covariance matrix. LKF has two tuning factors Q and R while RLS only has one λ. By selecting a good set of Q and R value, the estimation becomes fast and accurate. When Q is decreased, the estimation result will be more stable but follow the measurement data slower. Conversely, when R is decreased, the estimation result will follow the measurement data faster but be less stable. The effects of Q and R are shown in following two figures.

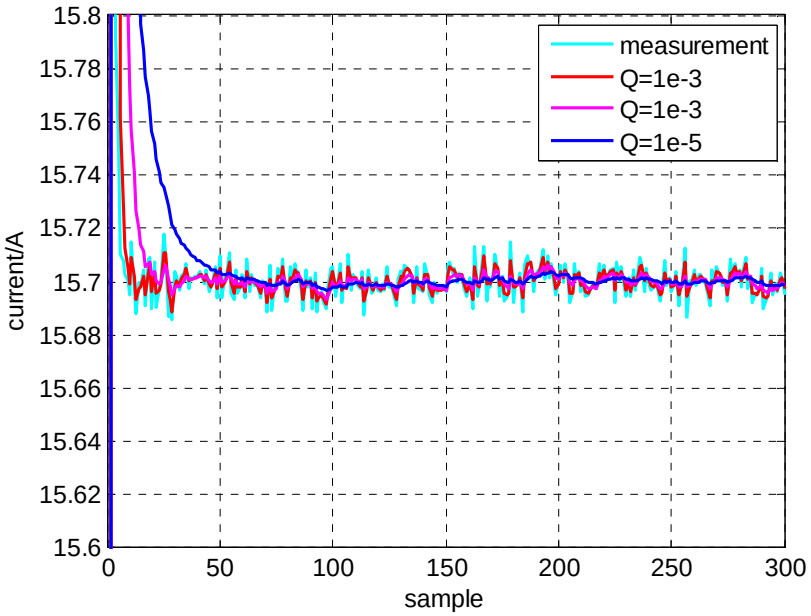

Figure 15: Effects of Q on errors

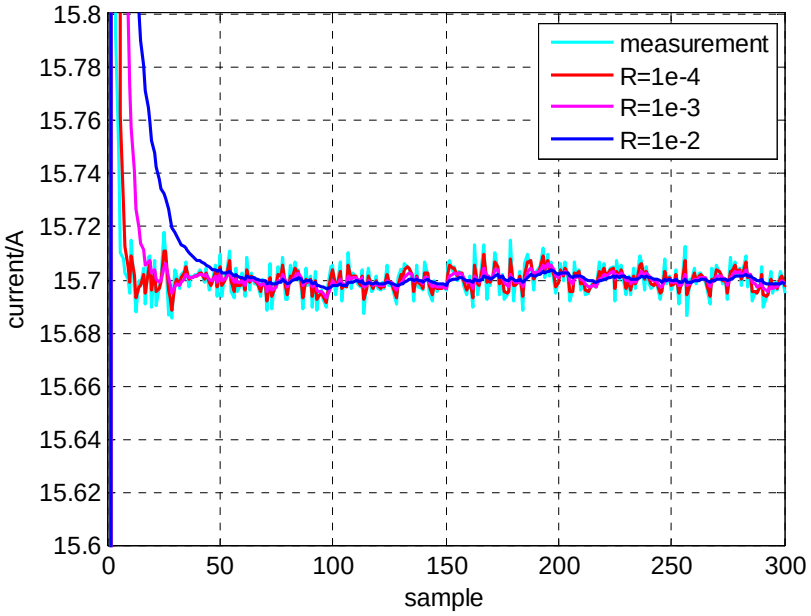

Figure 16: Effects of R on errors

In practice, the values of Q and R are determined based on stability of parameters estimation and errors of terminal voltage. Basically, the values of Q and R can be adapted dependent upon speed of changing parameters and the level of noises that should be removed. Several sets of the values have been applied for this battery dependent upon six current profiles under CC mode. The profiles are charging- resting, resting-charging, charging-discharging, discharging-resting, resting-discharging and discharging-charging. The values of Q and R used in the experiment is shown in Table 2. However, other combination of two values can deliver the similar results as well.

Table 2: Table of Q and R values

Profiles	Q	R
Charging-resting	diag([0.1 0.1 0.01 0.01 0.01])	0.01
Resting-charging	diag([0.5 0.5 0.02 0.02 0.02])	0.1
Charging-discharging	diag([0.01 0.01 0.01 0.01 0.01])	0.01
Discharging-resting	diag([0.05 0.05 0.01 0.01 0.01])	0.01
Resting-discharging	diag([0.5 0.5 0.02 0.02 0.02])	0.01
Discharging-charging	diag([0.05 0.05 0.01 0.01 0.01])	0.1

2.3.4. Validation of Parameters Identification

2.3.4.1. Simulation Validation

Before implementing these identification process into real experiments, these two approaches have been evaluated by simulation using the first order and second order ECM and

Simulink. In the first order ECM, the OCV part is excluded, so the model only contains a resistor and one set of RC circuit, as shown in Figure 17.

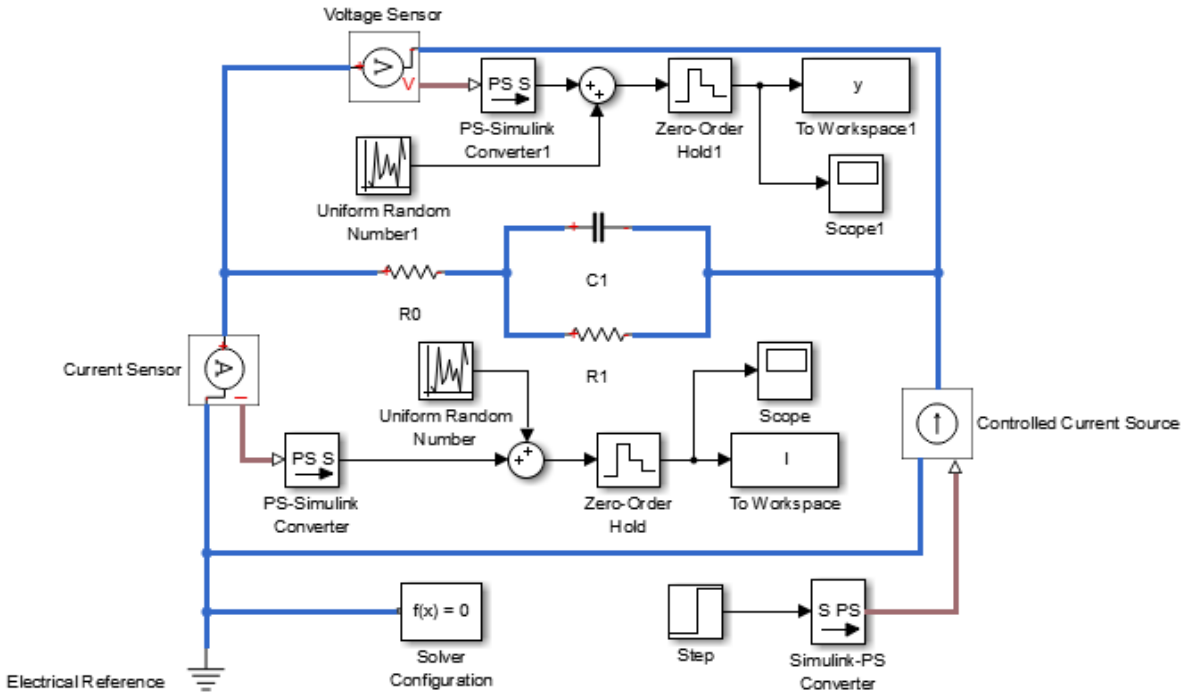

Figure 17: Simulink model of first order ECM

The predefined parameters in the first order ECM are:

$$R_0 = 8 \times 10^{-3}\Omega \quad R_1 = 8 \times 10^{-3}\Omega \quad C_1 = 500F$$

A step current input is applied to the first order ECM system, where the direction of positive current is discharging. Then there should be a voltage drop corresponding to a positive current. The current input and voltage response are shown in Figure 18:

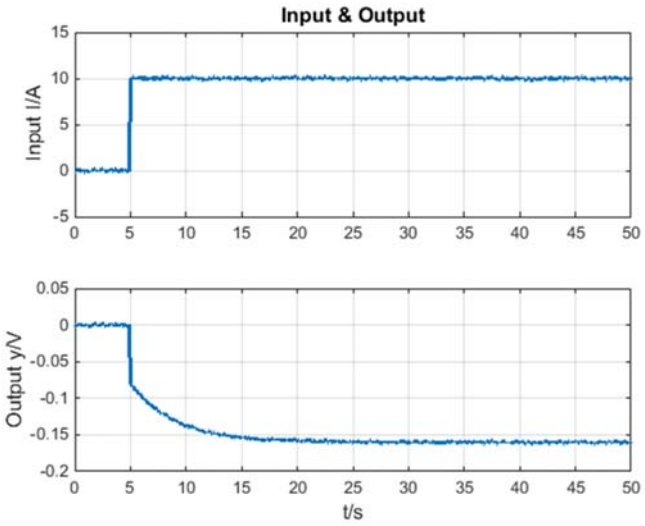

Figure 18: Input and output of a first order ECM system

In this simple system, all three techniques (including nonlinear Least Squares, Recursive Least Squares, and KF) are applied to estimate its parameters. The results are shown in Figure 19:

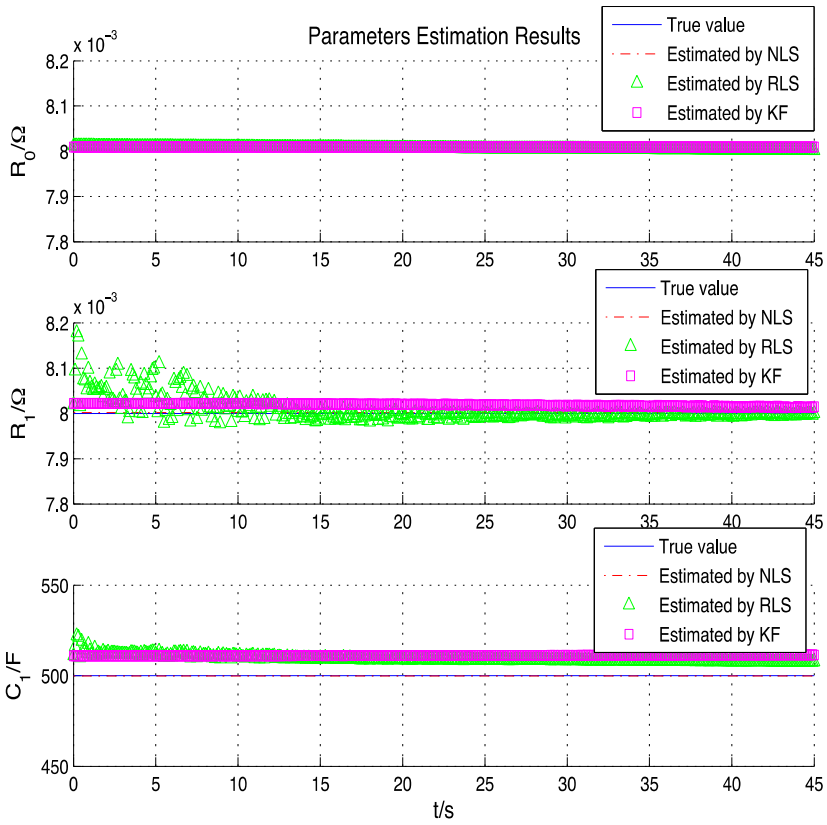

Figure 19: Parameters identification results of first order ECM system with a step input

As can be seen in the Figure 19, parameters that estimated by those three methods can all achieve satisfactory results. The nonlinear Least Square method is the most accurate way to estimate the parameters, but this method cannot be applied online due to the high memory required. The estimated parameters are also verified by comparing their response to the same input. The comparison is shown in Figure 20:

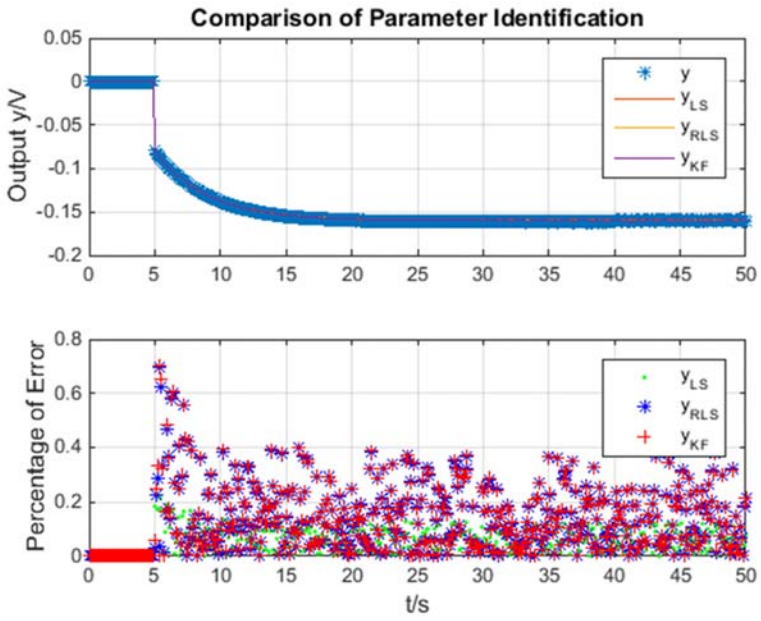

Figure 20: Validation of the estimated parameters

Then, another simulation is performed to compare RLS and KF for estimation of varying parameters, because those parameters in reality also vary, and are changing with several factors, including SOC, temperature, aging conditions, and direction of current. In this simulation, R_0 and R_1 are changing with time while C_1 still keeps at a constant value. Input is also changed to a repeating stair function. The input and output of this system is shown in the Figure 21:

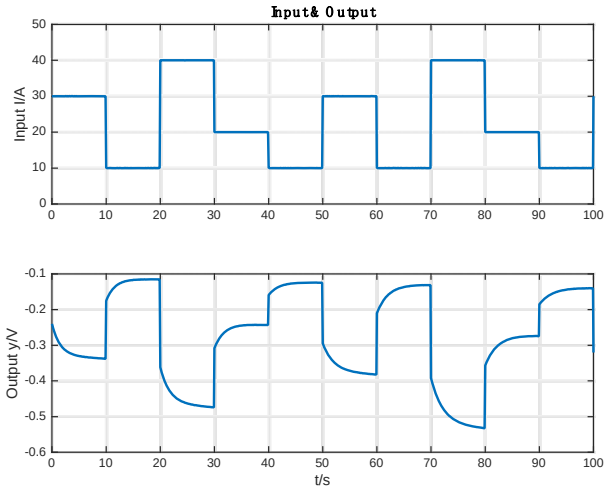

Figure 21: Input and output of the repeating stair function

The estimated parameters are shown in Figure 22

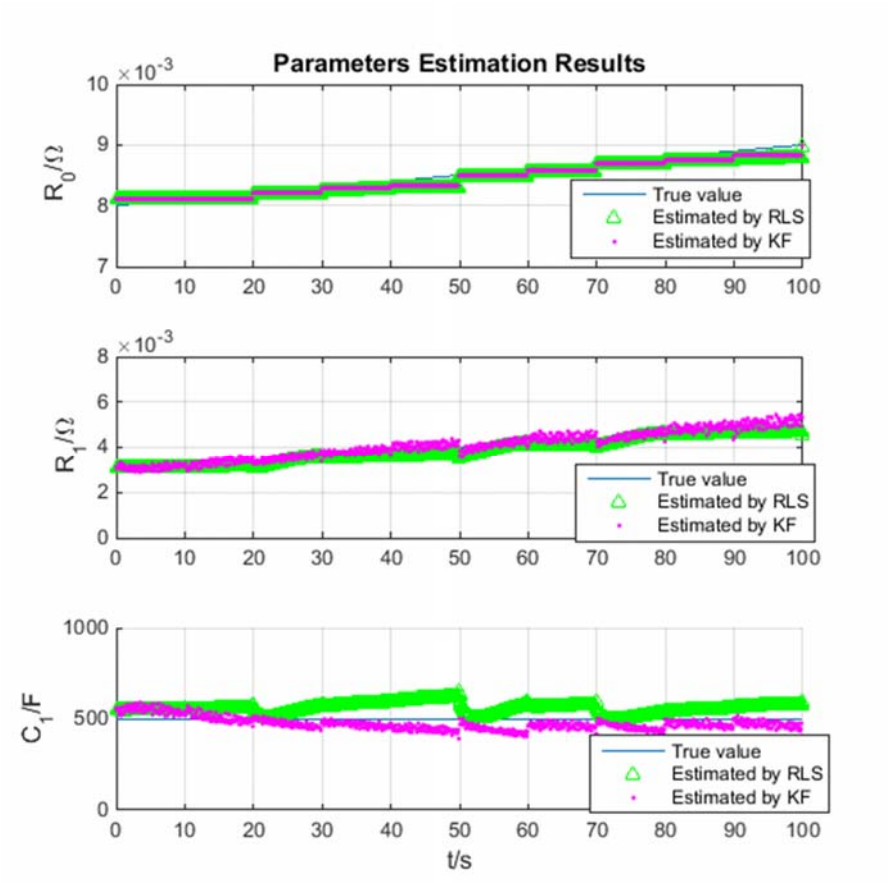

Figure 22: Parameters identification results of first order ECM system with varying parameter

The responses using estimated parameters are compared by simulation as shown in Figure 23:

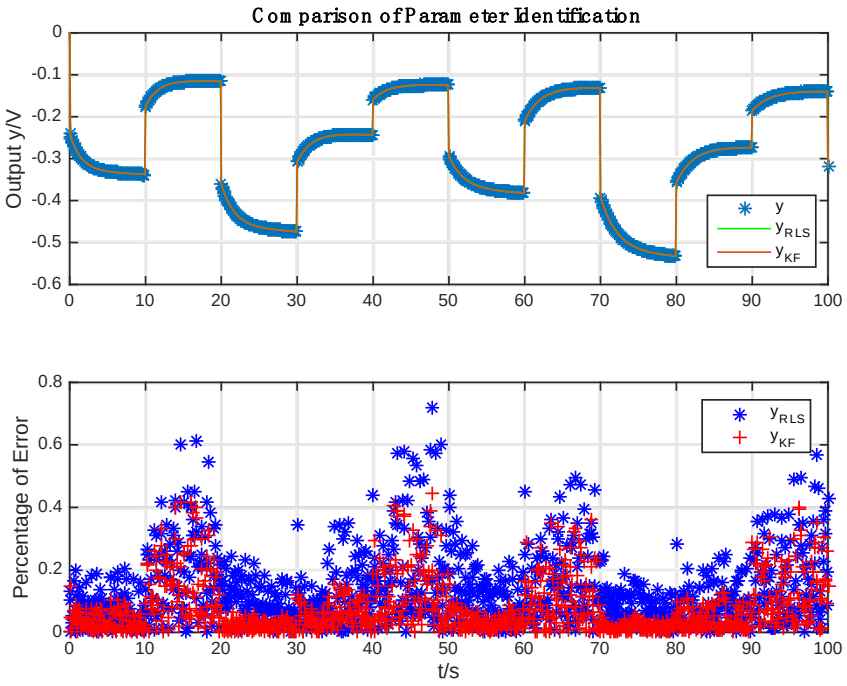

Figure 23: Validation of the varying parameters

In comparisons, both of RLS and KF show similar performances and can be used to estimate the parameters. However, KF is selected because of more flexibility in the tuning process. KF has Q and R that can be tuned to achieve satisfactory result while the RLS only has one tuning factor, which is the forgetting factor. Therefore, KF actually has a slightly better result than RLS in the estimation results.

The second order ECM system is also built using Simulink model. The OCV is added to the system in this improved system. The OCV is defined as a function of SOC, and the SOC is estimated by Ah Counting method. The simulation of a second order ECM is shown in following Figure 24

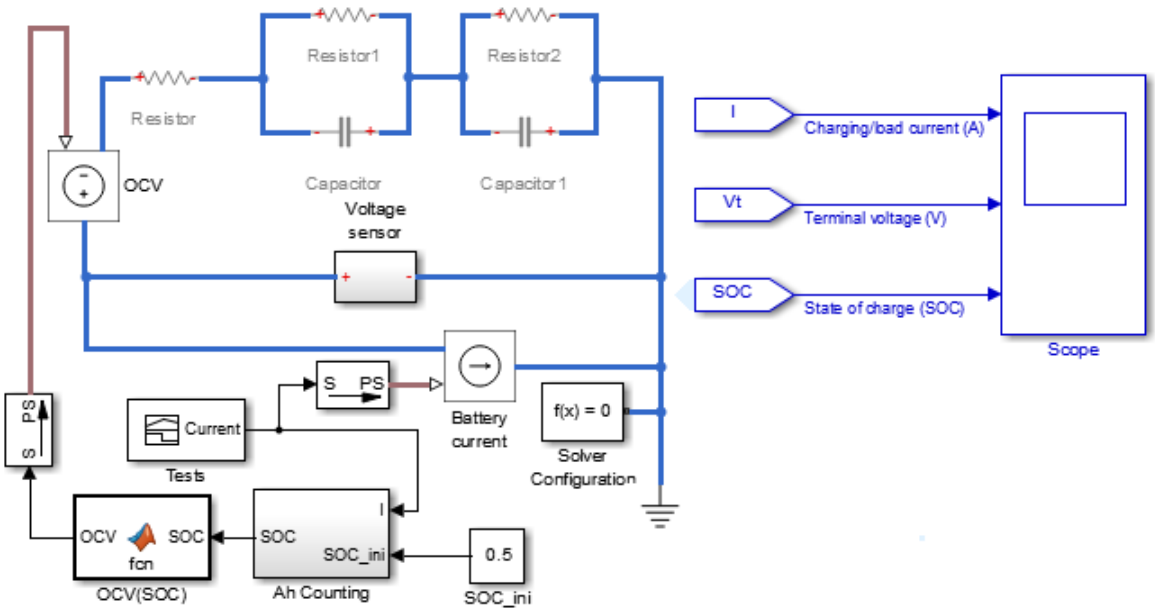

Figure 24: Simulink model of second order ECM

The true parameters in this Simulink model:

- $R_0 = 0.008\ \Omega$
- $R_1 = 0.05\ \Omega$
- $R_2 = 0.005\ \Omega$
- $C_1 = 2000$ F
- $C_2 = 2000$ F

A simple profile is applied to the second order ECM. The input current, output voltage, and SOC are shown in Figure 25

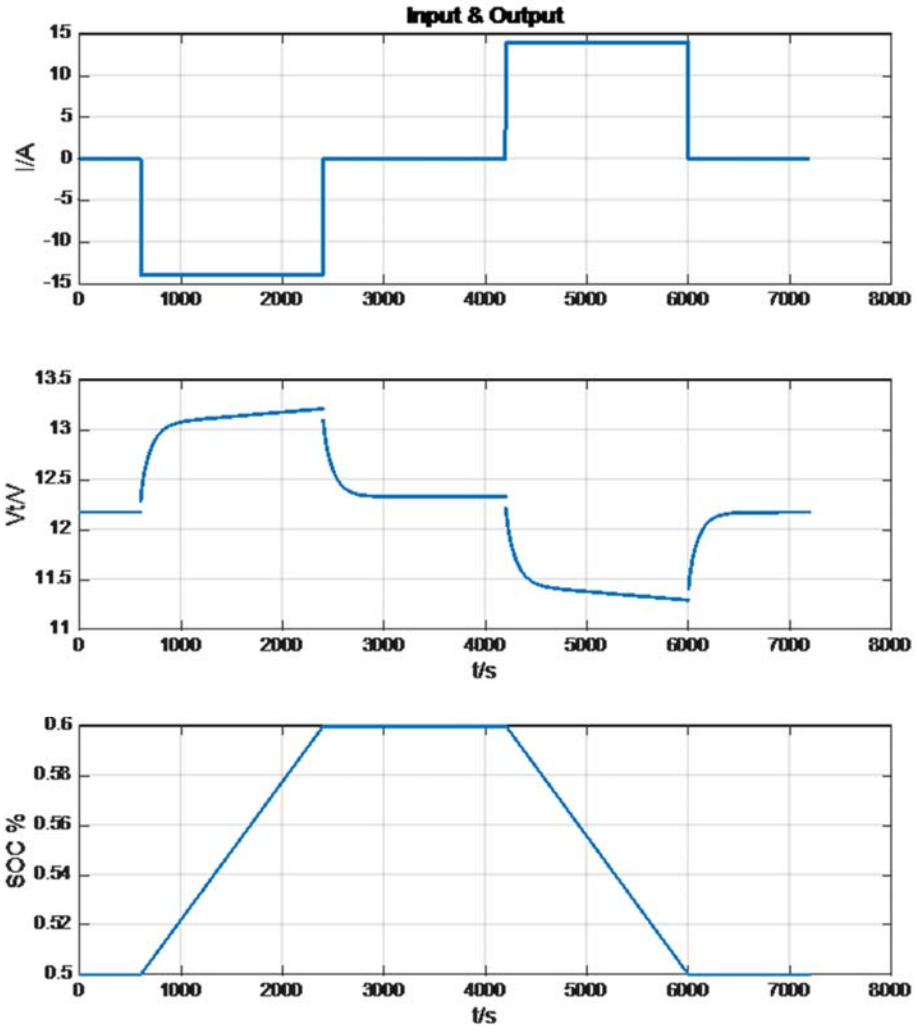

Figure 25: Input and output of the second order ECM system

There is no calculation at the beginning stage (both input and output are constants), since there is no excitation signal. The initial values of these parameters are estimated by Least Square method with the data collected in first 1000s data. The parameters are shown in Figure 26:

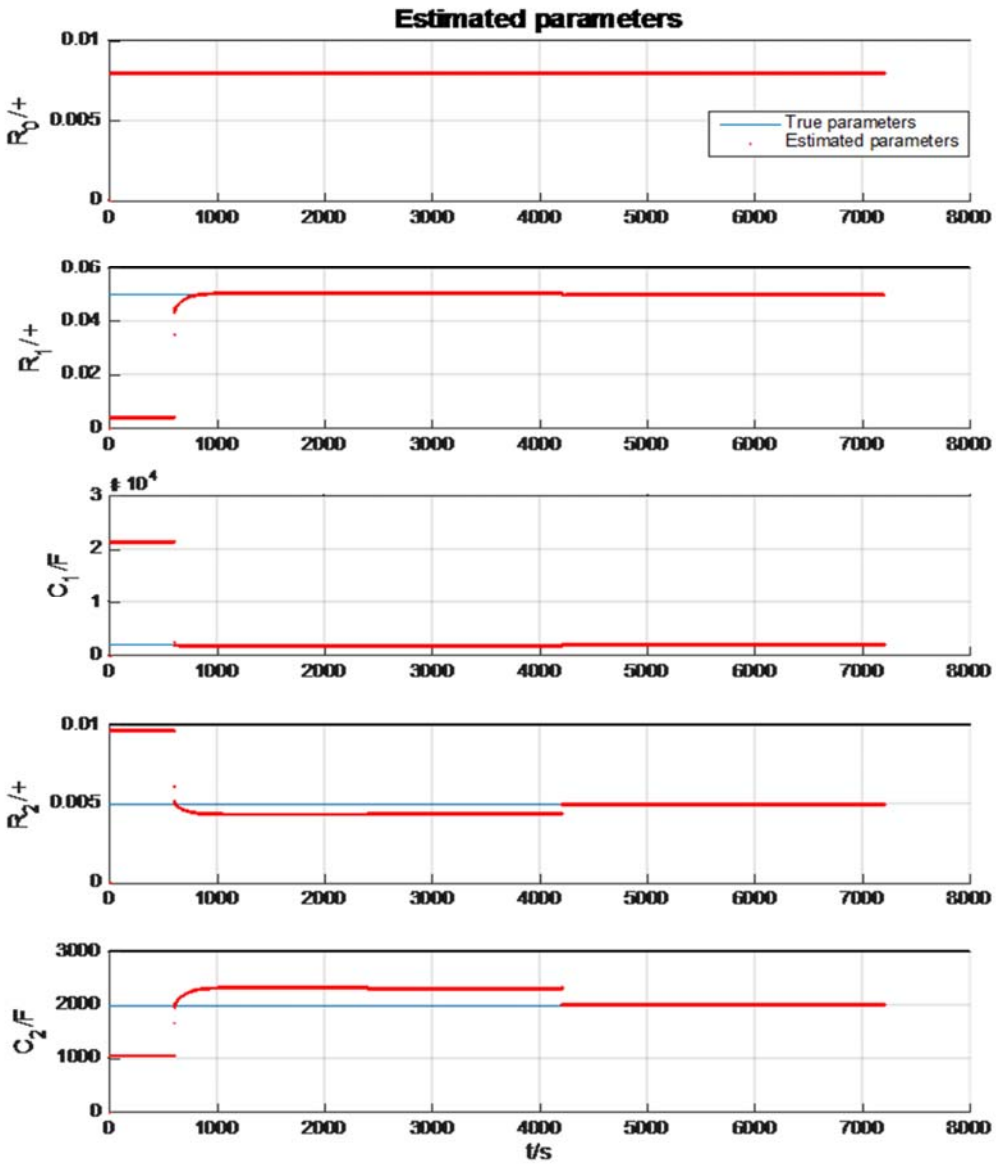

Figure 26: Parameters estimation results of second order ECM system

The estimated parameters can be validated by simulation of the response of the original input. This is shown in Figure 27:

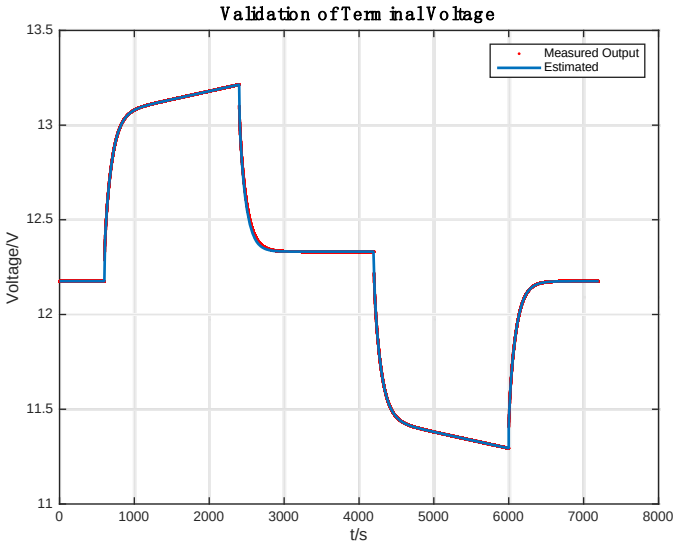

Figure 27: Validation of second order ECM

2.3.4.2. Experimental Validation

After the parameters identification method is evaluated by Simulation, I also applied those methods to some real experiments. Pulse discharging is applied to a fresh battery from 100% SOC to 0% SOC at a constant temperature of 25 $°C$. The input current and measured Terminal Voltage are shown in Figure 28.

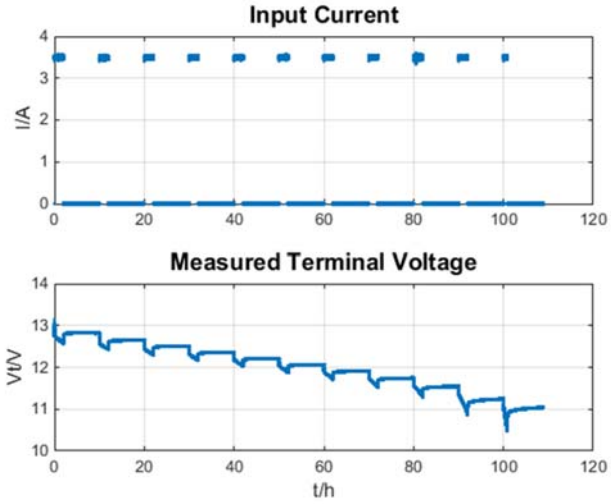

Figure 28: Input current and output voltage of experiment

The estimated parameters are shown as follows:

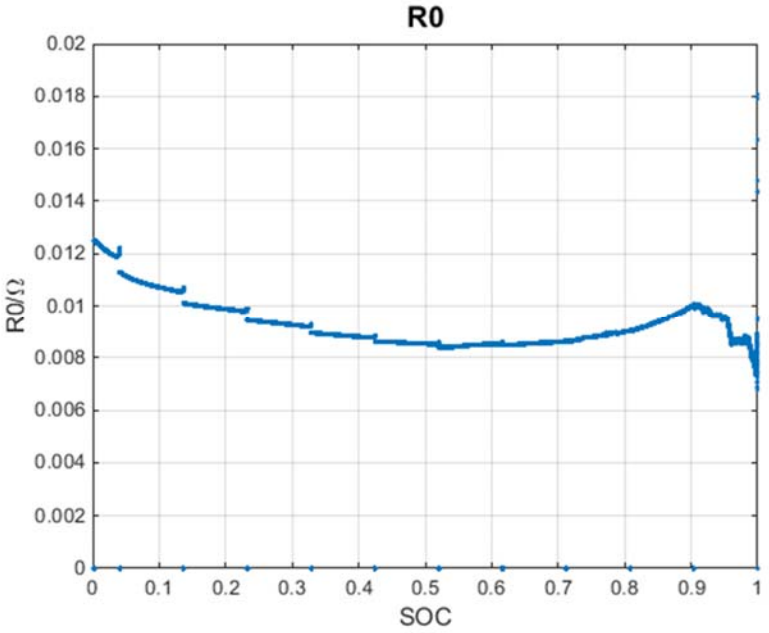

Figure 29: Estimated R_0 vs SOC

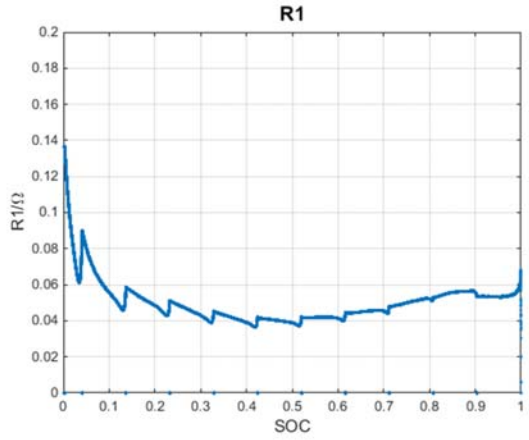

Figure 30: Estimated R_1 vs SOC

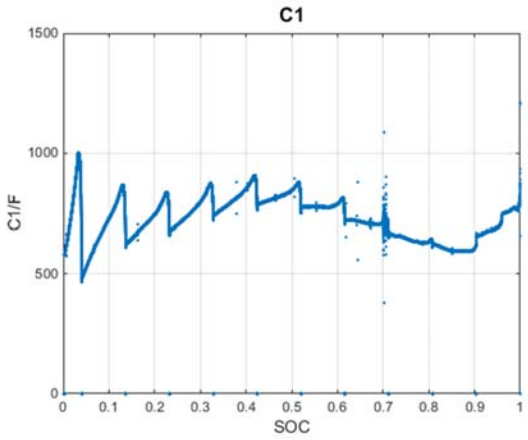

Figure 31: Estimated C_1 vs SOC

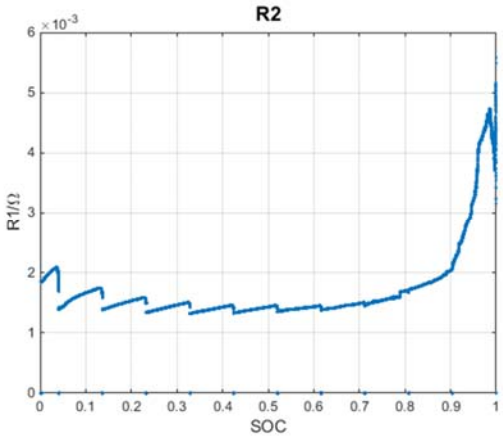

Figure 32: Estimated R_2 vs SOC

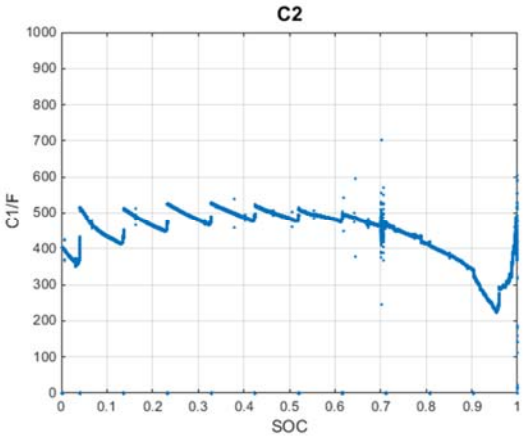

Figure 33: Estimated C_2 vs SOC

In order to validate this test result, I also used the estimated parameters to calculate the terminal voltage.

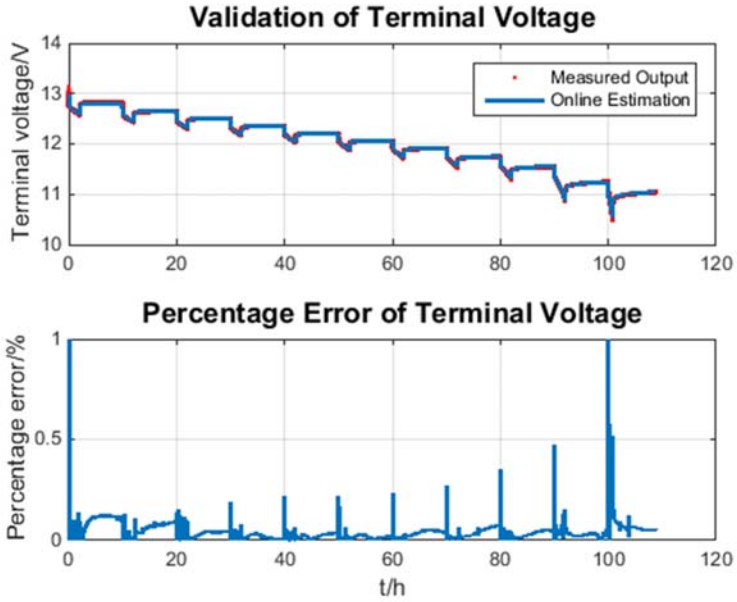

Figure 34: Validation of parameters estimated from experiment

2.4. Prediction of Available Power

2.4.1. Review of Methodology

The power capability of the battery should be limited in the safe operation range. The limiting factors include the terminal voltage, current, and SOC. Early researchers focused on the limit based on SOC, because it is easy to start and implement. Plett [23] mentioned one of these methods called rate limit based on SOC. It assumes that the present available energy, which is SOC, is a constant value and is estimated by SOC estimation techniques. Then, I can calculate the power of a battery over a certain time period by using the available energy divided by the time period. However, the amount of energy in a battery changes when the charging or discharging current is changing. It makes this method not accurate enough for immediate power estimation.

In order to avoid the assumption of constant energy in the first approach, recent researchers make use of the voltage limit in a battery to predict the battery's Available Power based on a model. This approach needs to identify battery's parameters first. Some researchers [19] propose a simple Ohmic's model, which only consist of a simple resistor and OCV. The problem is that it cannot simulate power for a certain period of time. Other researchers used first order or second order ECM to predict the Available Power. This method makes the power can be predicted in different time periods under consideration of temperature and aging effect. The only disadvantage is that it requires a high computational power. The major methods for calculation of SOH_P are shown in Table 3.

Table 3: Methods for calculation of SOH_P

Methods	Pros	Cons
Rate limits based on SOC [23]	• Simple • Low computation power • Suitable for long time power prediction	• Low accuracy • Update Q_{max} is required
Rate limits based on voltage with simple Ohmic's model [19]	• Simple • Low computational power • Accurate for instantaneous power prediction	• Cannot predict power for Δt seconds
Rate limits based on voltage with complex models [7] [22]	• Accurate • Good aging and temperature consideration	• High computational power

In addition, there are other methods that used experiment to find out the power capability. Parity-relation is one of these methods [20]. During cranking, there is a significant voltage loss. It looks at this cranking behavior of a lead acid battery, and builds a relationship with aging condition. This behavior is more reliable than a simple Ohmic's model, because experiments indicated that there is a linear relationship between voltage and current in the same condition. This is shown in following figure 3:

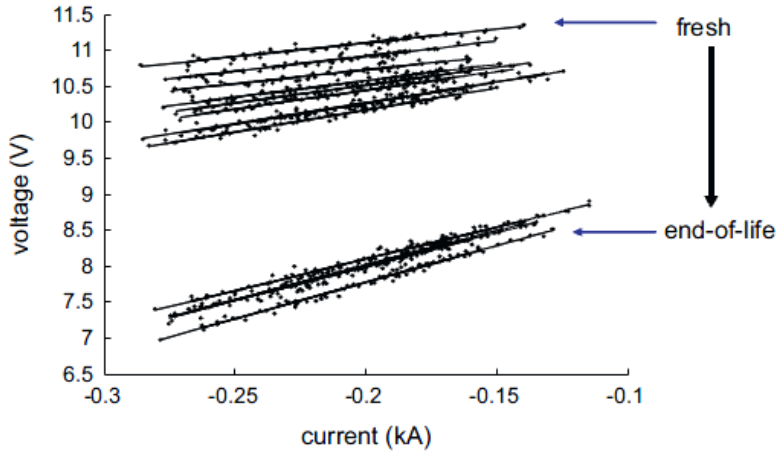

Figure 35 [20]: Typical voltage vs. current plot of a battery during cranking

The voltage estimated by the parity relation model may have a discrepancy with the real measured terminal voltage. This discrepancy is defined as the residual. Then, a pre-defined threshold is used to evaluate its performance. The result also needs to consider the effect of SOC and temperature. The whole process is shown in Figure 34:

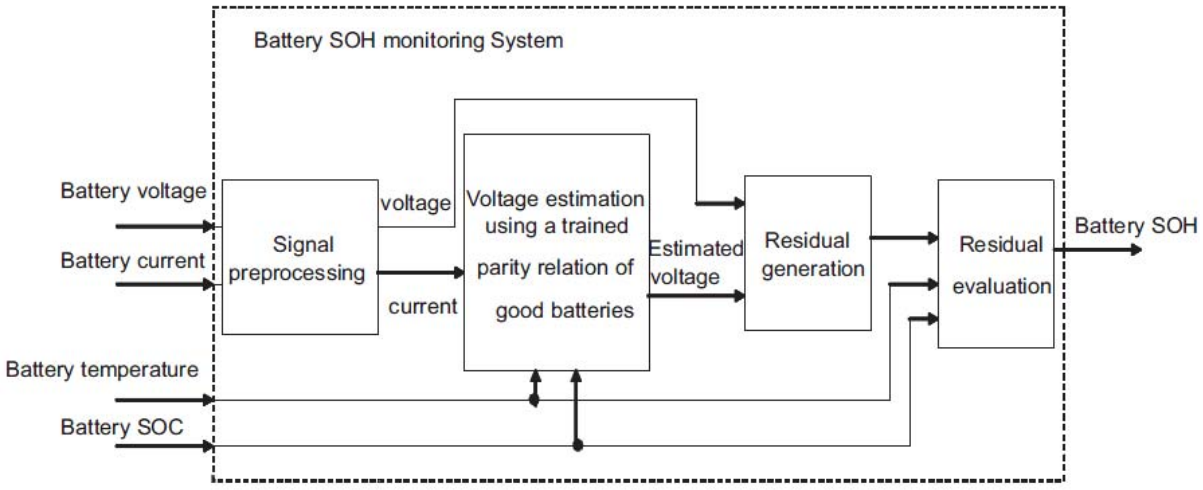

Figure 36 [20]: Complete process of parity-relation-based method

2.4.2. Approaches to Predict Available Power

The Available Power of battery is not easy to measure directly. It is common to predict the maximum current and multiply the predicted current with voltage limit instead. In real life application, constant current is the most common current profile. Thus, the charging and discharging current are assumed to be constant during the prediction period. This can greatly simplified the prediction process. Generally, the prediction period is up to 10 second. Since the prediction period is relatively short, simple approach only predicts the instantaneous power and assume the power is a constant during the prediction period. On the other hand, some advanced techniques can predict the power over certain period of a time. These methods are more accurate and are used in some application that requires a high precision.. This section discusses these in detail.

There are four approaches that can be used for on-line prediction of available charging and discharging power. The first one is based on characteristic map. This approach needs a lot of pre-measurement information and try to build a relationship between them. It is not discussed here. The second method is based on State of Charge (SOC) while the last two are based on terminal voltage of battery. This thesis analyzes the pros and cons of these three approaches and select the best one.

2.4.2.1. Rate Limits Based on SOC

The first approach is called Rate Limits Based on SOC. This approach assumes the energy stored in a battery is a constant value. The current energy level can be represented by the value of SOC. For a constant current I, current and SOC has the following relationship:

$$SOC_{k+1} = SOC_k + \frac{\int_k^{k+1} I\,dt}{3600 Q_{\max}} \quad (71)$$

, where the SOC_k is the present SOC, SOC_{k+1} is the predicted SOC after charging or discharging for a certain period of time in the future, Q_{max} is the Maximum Capacity in ampere-hour, and I is the current (assume positive value for discharging and negative value for charging).

If SOC is defined in a certain limit such that SOC_{min} (usually is 0) < SOC < SOC_{max} (usually is 1) for a battery. For a constant current, the integration part $\int_k^{k+1} I\,dt$ in the previous equation can be replaced by $\Delta t \cdot I$. Through a simple algebra, the following two equations can be derived:

$$I_{\text{maximum discharging}} = \frac{SOC_{\max} - SOC_k}{\Delta t} 3600 Q_{\max} \quad (72)$$

$$I_{\text{minimum charging}} = \frac{SOC_{\min} - SOC_k}{\Delta t} 3600 Q_{\max} \quad (73)$$

After current is predicted, the available charging and discharging power can be calculated by the following two equations:

$$P_{\text{maximum discharging}} = V_t \cdot I_{\max} \quad (74)$$

$$P_{\text{maximum charging}} = \left| V_t \cdot I_{\min} \right| \quad (75)$$

, where V_t is the terminal voltage of a battery, I_{min} is a negative value so the absolute value of it is taken.

This approach is very simple and can predict the Available Power for any time period. However, there are two key issues.

It is assumed that the energy stored in the battery is a constant value. While the Maximum Capacity changes very slowly and can be assumed to be a constant, the amount of energy can be released or absorbed will change when the current changes. More specifically, a high discharging

current reduces the amount of energy that can be released, and a high charging current reduces the amount of energy that can be absorbed. Thus, the prediction accuracy will be low when the absolute value of current is high.

The other issue is about the accuracy of SOC estimation. Since this approach requires a present SOC as an input, the estimation of SOC should be accurate to ensure accurate power prediction.

2.4.2.2. Rate Limits Based on Terminal Voltage

The other two approaches are discussed in this section. While the first method is based on a simple model, the second approach is based on a complicated model.

Both of these two approaches do not need the previous inaccurate assumption that the stored energy in the battery is a constant value. Conversely, these methods are based on the very important limitation on the terminal voltage. There is a terminal voltage drop during discharging. This voltage decreases when the discharging current increases. In order to protect the battery from reaching to a low terminal voltage level, a minimum value is specified for a battery. The maximum discharging power is the one when the terminal voltage reaches this specified minimum value. At same time, the current also increases to a maximum value. Since the available discharging power is a product of terminal voltage and current, the maximum available discharging power can be expressed as a product:

$$P_{\text{maximum discharging}} = V_{t,\,\min} \cdot I_{\max} \qquad \textbf{(76)}$$

Similarly, the terminal voltage increases during charging and a maximum terminal voltage is specified for a battery. The maximum charging power is the one when the terminal voltage

reaches its maximum value and charging current reaches its minimum value (the sign of the current at discharging is negative). Thus, the maximum available charging power can be expressed as:

$$P_{\text{maximum charging}} = \left| V_{t,\,\max} \cdot I_{\min} \right| \quad (77)$$

The specified minimum and maximum terminal voltage are fixed values, so the prediction of available charging and discharging power can be obtained by finding out the maximum current that makes the terminal voltage to reach its maximum or minimum specified values.

2.4.2.2.1. Zeroth Order Randles' Model

The first method makes use of the simple Ohmic's model. R_0 represents the internal resistance of battery that is used to simulate the immediate voltage drop when a constant current is applied.

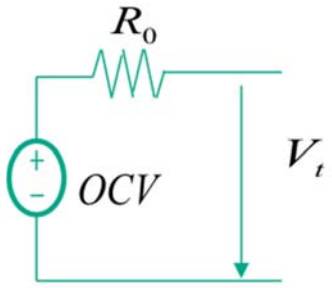

Figure 37: First order ECM

The dynamic resistance of battery can be expressed as:

$$R_{\text{internal resistance}} = \left| \frac{\Delta V_t}{\Delta I} \right| \quad (78)$$

In the prediction process, the initial current is zero and the initial terminal voltage is the same with the open circuit voltage (OCV). OCV is a function of SOC, which relationship is already known. The Kalman Filter can be used to estimate SOC, so the value of OCV can be calculated. Since the maximum Available Power is the one when the terminal voltage reaches the design limits,

the final voltage is the terminal voltage limits. The internal resistance is estimated in the parameters identification process. Thus, the only unknown in the equation is the final current and can be predicted in equation **(79)**..

$$I_{predict} = \frac{OCV - V_{t,\,set}}{R_0} \qquad \textbf{(79)}$$

, where $V_{t,\,set}$ is equal to the minimum terminal voltage in discharging or the maximum terminal voltage in charging.

This approach is also very simple and only requires a low computational power. Thus, it can be easily implemented into the microcontroller. Moreover, it is accurate for instantaneous power prediction, but prediction during a period is not possible.

2.4.2.2.2. Second Order Randles' ECM

The last approach is based on a second order Randles' ECM to simulate the Available Power.

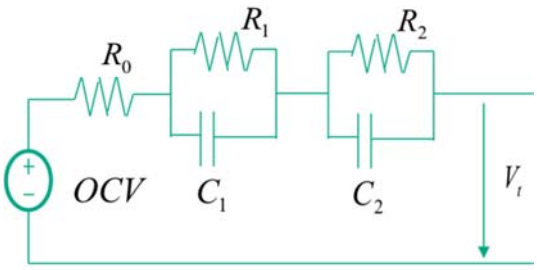

Figure 38: Second order ECM

The parameters (R_0, R_1, R_2, C_1, and C2) are estimated in the parameters identification process. OCV can be calculated by the using the estimated SOC and the known relationship between OCV and SOC. If I input a current into this model, the terminal voltage response of the corresponding current can be calculated by iterative process, so an optimum current that can make

the terminal voltage equals to the voltage limit can be obtained. Flowchart for this iterative process is shown in Figure 39.

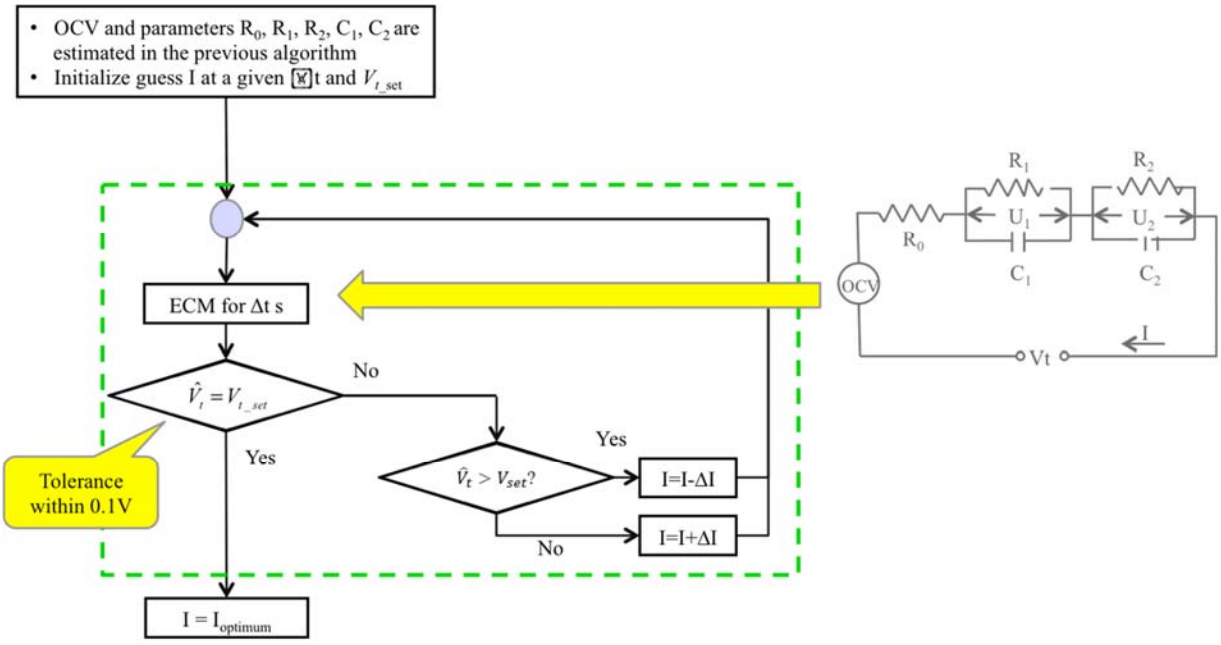

Figure 39: Flow chart of Available Power Prediction

The second order ECM not only can represent the immediate voltage response of a battery, but also be used to predict the voltage response for 10 seconds or 20 seconds. Although the parameters and OCV may change for a long time charging or discharging, they can be assumed to be constant during the prediction process. Thus, it is possible to predict the power for 10 seconds accurately, which is the typical longest period required for vehicle applications. The only disadvantage of this approach is the calculation time needed for iteration.

2.4.3. Experimental Validation of Power Prediction

The standard power measurement method uses Hybrid Pulse Power Characterization (HPPC) cycle that is commonly used for Lithium ion battery. However, it cannot be applied to

lead acid battery because HPPC requires a setting for current limitation, but there is no current limitation for a Lead acid battery in a vehicle. Thus, I propose a different way to measure the maximum Available Power.

The immediate power is a product of the terminal voltage and the current. For calculation of the average power over a certain period, the immediate power over time is integrated and then divided it by the period. In the power prediction process, I have specified that the current should be constant value. Based on the power calculation formula above, the power at certain current can be measured. This power is the actual measured power at a certain current, SOC, and temperature. In order to measure the maximum Available Power, the absolute value of current was gradually increased by checking if the terminal voltage is still within the limitation. When the terminal voltage is close enough to the limit, the average power at this current is the maximum available charging or discharging power. Comparison between measured and estimated power is shown in Figure 40 .

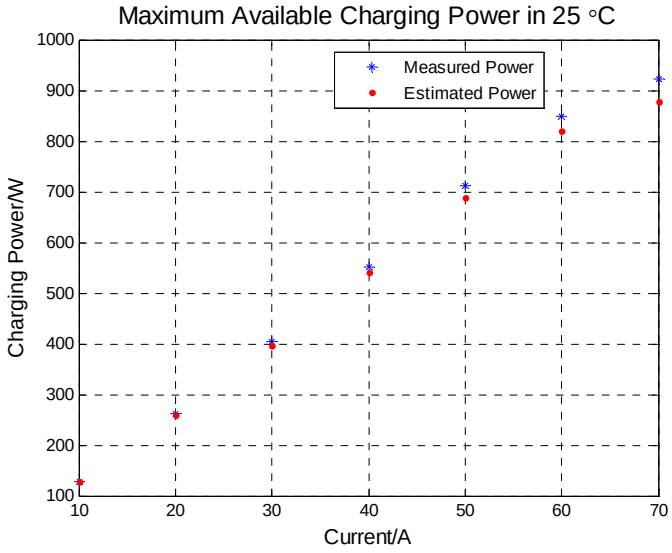

Figure 40: Comparison of measured and estimated available charging power

This method is also used for aging experiments. Predefined aging cycles are applied to a fresh battery at constant temperature of 25 $°C$. I measured the maximum available discharging power at 50% SOC and compared it with the proposed Available Power prediction method. The maximum available discharging power around 50% SOC at 25 $°C$ is plotted in Figure 41.

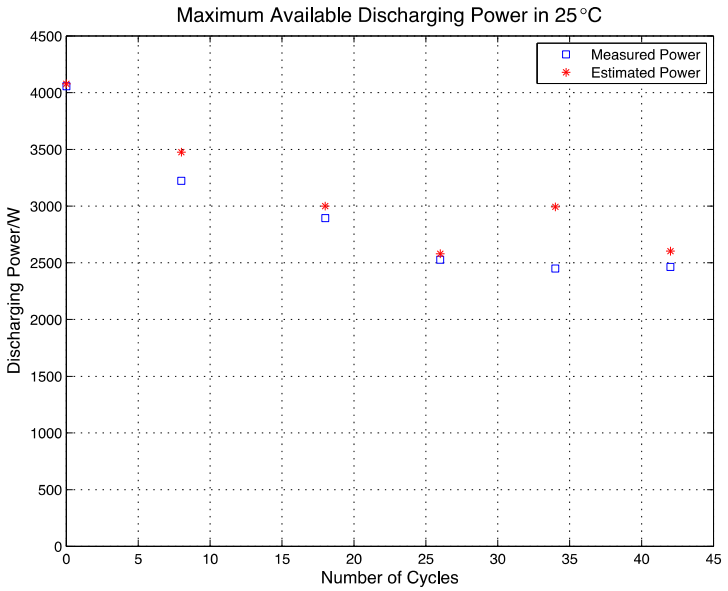

Figure 41: Experimental validation of power prediction method in aging condition

3. Maximum Capacity Estimation

3.1. Review of Methodology

Capacity is the capability of batteries to store energy. The maximum amount of energy that a battery can store at present condition is defined as the Maximum Capacity of the battery. The value of capacity is usually expressed in ampere hours (Ah). This value only varies slightly for individual battery or cell of a given type due to production tolerances, but it changes significantly in different temperature and aging conditions. There is a standard offline process to measure Maximum Capacity, where the discharging energy is measured by applying a constant current in a predefined temperature. However, the measured capacity varies dependent upon current or temperature and is significantly reduced when a battery ages.

Here are the steps for measurement of Maximum Capacity at 25 $^{\circ}C$:

1) Apply a 25A constant discharging current to the battery until the terminal voltage reaches 10.5 V
2) Rest the battery for 6 hours
3) Apply a -14 A constant charging current to the battery until the terminal voltage reaches 14.3 V
4) Change to a constant voltage charging until the total charging time is 24 hours
5) Rest the battery for 12 hours
6) Apply a 3.5 A constant discharging current to the battery until the terminal voltage reaches 10.5 V

In step 6, the total energy that can be released is defined as the standard value of Maximum Capacity.

There are several approaches to estimate Maximum Capacity of batteries. The first one, such as [33], is based on a relationship between parameters and capacity, which disadvantageously requires a lot of experiments and the result has very limited usage in aging condition because this relationship changes when batteries age.

Singh [34] proposed using fuzzy logic to determine the Maximum Capacity. Fuzzy systems translate the behavior of the system into fuzzy sets and by using rules based on a linguistic representation of export knowledge to process the fuzzy data. Then, Fuzzy logic data analysis is used to estimate the Maximum Capacity of a battery directly from measured battery data without any intermediate transformation steps. There are some typical conceptual components for fuzzy system:

- A rule base describing the relationship between input and output variables
- A data base that defines the membership functions for the input and in the case of Mamdani modeling output variables
- A reasoning mechanism that performs the inference procedure
- A de-fuzzification block that transforms the fuzzy output sets to a real valued output

Pascoe [35] introduced a method based on Coup de Fouet. It is the correlation between battery's Maximum Capacity and parameters found within the voltage profile during the initial stages of discharging. The following Figure 42 shows this region:

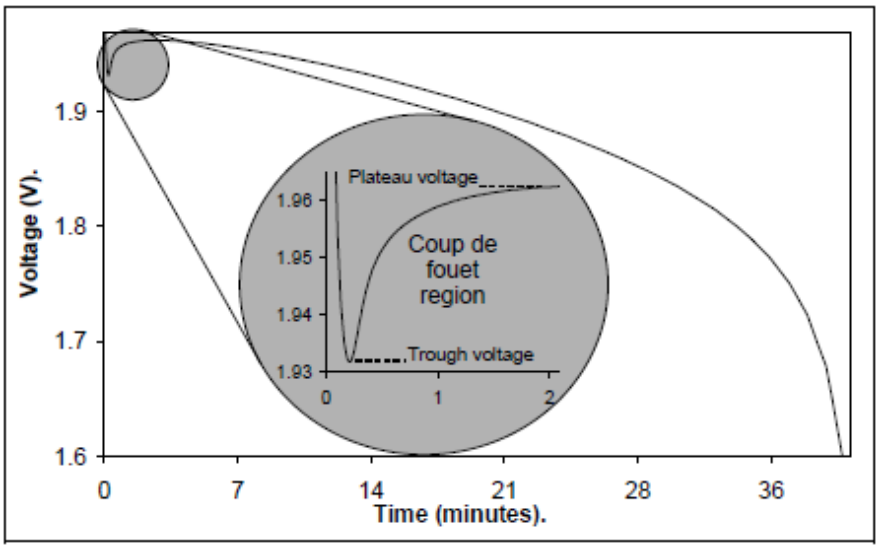

Figure 42 [35]: Coup de Fouet region in a discharging curve

Coup de Fouet is a special electrochemical phenomenon in a lead acid battery. Although there is no clear explanation of this effect, it does have a certain relationship with the capacity of a battery. There are two approaches for this method. One approach is based on a fixed operation condition, and compares this region with a fresh battery. This method is easy to implement online, but it requires a certain condition of current rates and temperature that can be compared with a fresh battery. The other approach is applying correction factors so that the test can be conducted in different operation condition. However, this requires extra experiment and may also need to change these factors in different aging condition.

The last approach is based on the definition of SOC (see equation **(21**)), which can be used to calculate the SOC with a known Maximum Capacity value. When the SOC is estimated by other methods, this equation can be used to estimate the Maximum Capacity. The key issue involved in this approach is the estimation of SOC or OCV. If OCV can be estimated, the SOC can be calculated based on OCV-SOC curve, which is pre-measured. After SOC or OCV is estimated, a

variety of methods can be used to estimate the Maximum Capacity based on **(21)** and are summarized in Table 4:

Table 4: Methods for Maximum Capacity estimation based on definition of SOC

Methods	**Pros**	**Cons**
Based on terminal voltage of resting	• Simple implementation • Long estimation period	• Blind current may exist and cause inaccuracy
Based on an observer [36]	• Simple • Stable	• Requires accurate SOC estimation
Based on RLS [37]	• Stable • More accurate than an observer	• Requires accurate SOC estimation
Based on dual KF [4]	• Co-estimation of SOC	• Results may be divergent
Based on joint KF [38]	• Co-estimation of SOC	• High computational power

3.2. Approaches to Estimate Maximum Capacity

This thesis proposes using the approach based on the definition of SOC to estimate Maximum Capacity. The core idea is based on the change of SOC in different aging condition. If I discharge a same amount of energy for a fresh battery and an aged battery, the change of SOC is different. Then, I can use this difference of SOC to estimate the Maximum Capacity. This approach assumes the SOC estimation is accurate and not based on Coulomb Counting. The estimation of SOC is discussed in my group mate's thesis.

I use one simple calculation to illustrate the basic idea in details. It is known that the OCV is equal to the terminal voltage after the battery is rested for enough time. If a simple constant current discharging profile is applied to the battery, I can know the OCV at initial and end state. Then, the SOC can be calculated based on the pre-measured OCV-SOC curve. In order to estimate the Maximum Capacity, I reformulate the equation **(21)** into equation **(80)** under consideration of SOC at k-1 step.

$$SOC_k - SOC_{k-1} = -\frac{\int_{k-1}^{k} Idt}{3600 Q_{\max}} \qquad \textbf{(80)}$$

Q_{max} is given as follows:

$$Q_{\max} = -\frac{\int_{k-1}^{k} Idt}{3600\left(SOC_k - SOC_{k-1}\right)} \qquad \textbf{(81)}$$

This simple approach reveals the basic idea how to estimate the Maximum Capacity. A battery is simply discharged with a constant current for a certain time and the terminal voltage is measured before and after discharge. Since the OCV is equal to terminal voltage after the battery rest for enough time, the value of OCV before and after the discharging can be obtained. The OCV-SOC curve measured previously can be used to calculate corresponding SOC before and after the discharging. When the k-1 step and k step are the instant before and after application of the discharging current, respectively, the max capacity can be estimated by applying the equation **(81)**.

This one step calculation may not be accurate, because there are always some errors in both of the integration of current and SOC estimation. It is better to consider several steps and minimize these errors with an estimation technique, such as Kalman Filter or Least Squares. Particularly, attention should be paid to two errors. The first one is by the longtime current integration that may deliver a biased result. Even if a very high-resolution current sensor is used, there might still exist

a small error. The error gradually builds up during the long time charging or discharging. Thus, the time step of SOC_k and SOC_{k-1} should be short. Moreover, it is also important to pay attention on the errors in SOC estimation. There is always some error in SOC estimation no matter whatever approaches are applied. Moreover, SOC may not change in a short time, so the time step of SOC_k and SOC_{k-1} should be large enough. A long time step can minimize the effect of errors in SOC estimation, because the Maximum Capacity estimation only cares about the difference of SOC_k and SOC_{k-1}. Thus, the selection of sample time should consider both of two factors.

For estimation of Maximum Capacity, RLS method is used. I propose to collect next SOC values only when the SOC change is larger than 5%, since SOC values may not change much in one sample time and the current is not large enough to change the SOC in a short time. After collecting several data, RLS method is applied in equation **(68)** to get the current Maximum Capacity of the battery. The estimation model is shown below:

$$\underbrace{SOC[k] - SOC[k-1]}_{y} = \underbrace{\int_{k-1}^{k} Idt}_{\varphi^T} \underbrace{\frac{1}{3600 Q_{\max}}}_{\theta} \qquad \textbf{(82)}$$

There are several reasons for choosing this approach. The first reason is that the Maximum Capacity does not change in a short time. It may need a month to change 1 Ampere-hour in real vehicle. Thus, Maximum Capacity does not need to be estimated very frequently. Secondly, the requirement for resolution of Maximum Capacity is very low. Resolution of 1 Ampere-hour is enough for all other applications. Lastly, this method can estimate the capacity in one step considering several data sets. It would greatly save time and calculation effort.

3.3. Experimental Validation of Maximum Capacity Estimation

Predefined aging cycles are applied to a fresh battery at 25 $°C$ until the capacity fades around 50%. The true capacity is measured by the standard method explained previously. Extended Kalman Filter is used to estimate the SOC continuously, and the SOC data is recorded only when the change of SOC is more than 5%. The current capacity between each SOC data was recorded. Then, RLS is used to found out the Maximum Capacity. The estimated capacity is also compared with the capacity measured with standard method. The result is plotted in Figure 43:

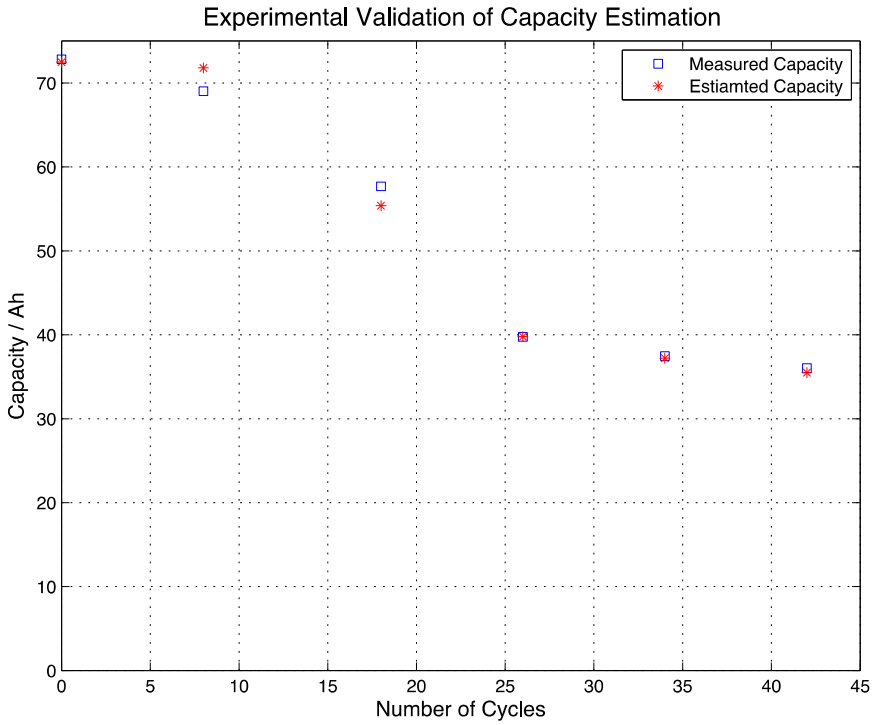

Figure 43: Experimental Validation of Maximum Capacity Estimation

4. Evaluation of SOH

4.1. Introduction of SOH

SOH is defined as the present conditions of a battery compared with the conditions of a fresh battery. It represents the abilities of a battery to store energy, source and sink high currents, and retain charge over extended periods [17] [39]. These abilities decrease over the battery lifetime due to aging. It is common to define the SOH is 100% for a fresh battery and SOH is 0% when one of these two capacities decreases to a minimum value. One thing should be pointed out is that the battery may still can be used when the SOH is 0%, because this is merely an indicator that reflects the battery has already reached to its predefined criteria for replacement.

The ability to store energy can be quantified as the Maximum Capacity of a battery. It is the maximum amount of energy that can be stored in a battery. The Maximum Capacity of a battery is gradually faded during its lifetime, and is defined as capacity fade or SOH_Q. When the capacity is not enough for its normal use, a battery should be replaced. The estimation of Maximum Capacity is a very challenging task, because it does not related to anything directly. Most researchers make use of the equation **(21)** to estimate the Maximum Capacity. This thesis has describe the details in Chapter 3.

The ability of source and sink high currents are the available discharging and charging power of a battery. This is measureable by a certain device and can be easily tested. It also gradually decrease during battery lifetime. I define this aging process as power fade or SOH_P. There is a direct relationship between Available Power and battery parameters. Thus, most of the researchers predict the Available Power based on battery parameters.

The last ability can be described as how much charge an aged battery can accept. It more or less related to its inner structures and it is hard to measure directly. Most researchers propose to use either SOH_Q or SOH_P to represent the value of SOH. On the other hand, other researchers tried to find a relationship between SOH and other conditions. The problem is that those methods can only be implemented in lab but is hard to integrate in a real vehicle. Thus, this thesis focuses on the Capacity Fade SOH_Q and Power Fade SOH_P of a battery.

4.2. Approach to Evaluate of SOH and Detect Battery Failure

I propose to evaluate the SOH considering both effects of power fade and capacity fade. The SOH is represented by two values: SOH_P and SOH_Q. SOH_P is defined as the present power capability divided by the nominated power capability of a fresh battery.

$$SOH_P = \frac{P_{present}}{P_{\text{nominated}}} \times 100\% \quad \textbf{(83)}$$

, where the $P_{present}$ is the present power capability at a certain condition and is predicted by Available Power prediction method, and $P_{\text{nominated}}$ is specified by manufacture for a fresh battery

The SOH_Q is defined as the present Maximum Capacity of battery divided by the nominal capacity of a fresh battery.

$$SOH_Q = \frac{Q_{\max}}{Q_{\text{nominated}}} \times 100\% \quad (84)$$

, where the $Q_{\max}$ is the Maximum Capacity of a battery at certain aging condition and is estimated by the capacity estimation method, and $Q_{\text{nominated}}$ is specified by manufacture for a fresh battery

The evaluation of SOH can also be used in a battery failure detection algorithm. It is because battery failure is a special case when either of SOH_P or SOH_Q becomes zero.

There are four criterions that defined the battery failures.

- Mechanical damage
  - When the voltage exceeds a certain limit (V_t>15.5V or V_t<9V), mechanical part of a battery can be damaged.
- Short circuit
  - When the battery's normal current is extremely high (I>200A) for more than 20s, a battery can be damaged
- Capacity fade
  - When the max capacity fades 50%, a battery can be failed
- Power fade
  - When the power fade 50%, a battery can be failed
  - The power fade is mainly due to the increase of internal resistance, and there is a proportional relationship between internal resistance and Available Power. Thus, when the internal resistance increase to 200% of its original internal resistance, a battery can be failed

The maximum Available Power prediction and Maximum Capacity estimation method are both very important for the determination of battery failure. Thus, the result of Available Power prediction and Maximum Capacity estimation are integrated into the determination of a battery failures.

5. Summary and Future Research

This thesis presents online approaches to predict Available Power and estimate Maximum Capacity. The Available Power during a given time is calculated using a maximum allowable current at a given limiting terminal voltage. To find out the maximum current, the terminal voltage is calculated iteratively using a second order Randles' ECM by incrementing the current until the voltage reaches the limited value. Then, the Available Power is obtained by multiplying the maximum current with the limiting terminal voltage. However, the parameters of the model vary continuously because of effects of amplitude of current, temperature, SOC in addition to ageing. Therefore, exact values of parameters are the crucial factor for accurate estimation of the power prediction, which is carried out by employing LKF based on ARX model. This method is verified by both simulations and experiments. The summary of contributions are shown as follows:

a. A thorough literature review of the current technologies of batteries parameters identification
b. Analysis of the advantages and disadvantages of zeroth, first, and second order Randles' ECM system. The performance of these systems is discussed based on their fitting result of a set of measured data. Second order ECM is selected because of the best fitting result.
c. Conversion of continuous system into discrete system by Taylor expansion and Laplace transform. The performance of these two methods is compared with the response of continuous system. The results are quite similar, but the conversion in time domain results in a simple equation and is finally is selected.

d. Two online methods to estimate parameters in ARX system are discussed and compared, including KF and RLS. Although RLS has fewer tuning factors and is simpler than KF, KF is selected as the final method to estimate parameters, since KF has a slightly better performance as compared with RLS
e. Three common approaches to predict Available Power are introduced. The method using a seconder order Randles' ECM is selected. The result is also verified by experimental data.

For estimation of the Maximum Capacity, I make use of the equation to estimate SOC in Coulomb Counting. If SOC is known, this equation can be used to estimate Maximum Capacity. This approach requires an accurate SOC estimation (less than 5%) that I used from a previous work of Dr. Choe's research group. I propose using RLS to minimize the error in SOC estimation. The result of Maximum Capacity estimation is validated in aging conditions.

This thesis also introduces a combined approach to evaluate the SOH of an AGM batteries, considering both Power fade, SOH_P and Capacity fade, SOH_Q. SOH is an indication for the health information of a battery, such as whether the battery should be replaced. Power fade requires the input from Available Power prediction while the capacity fade requires the input from Maximum Capacity estimation. Then, these input are compared with reference data of a fresh battery. In addition, power fade and capacity fade can also be integrated into the criterions to detect failure of batteries. When either power fade or capacity fade reaches to zero percent, they battery can be failed.

5.1. Future Research

a. In CV charging mode, the terminal voltage is very high and the chemical reactions in this condition are more complicated than the normal CC mode, such as water loss. There does not exist an appropriate model for CV charging, which can be addressed in the future work.

b. Parameters are also functions of current. The change of current only has a very limited effect to the parameters, so this effect can be ignored in the prediction of Available Power. However, if a more accurate power prediction is required, these effects should be considered into the prediction process.

c. When the capacity is very low, the OCV-SOC curve needs to be adjusted. This change is measured offline and input into the capacity estimation process. However, future research may develop an advanced approach that can estimate this relationship online.

Reference:

[1] Y. Barsukov and J. Qian, Battery power management for portable devices, Texas: Artech House, 2013.

[2] P. Delahay, M. Pourbaix and P. Van Rysselberghe, "Potential-pH Diagram of Lead and its Applications to the Study of Lead Corrosion and to the Lead Storage Battery," *Journal of The Electrochemical Society,* vol. 98, no. 2, pp. 57-64, 1951.

[3] G. L. Plett, "Sigma-point Kalman filtering for battery management systems of LiPB-based HEV battery packs: Part 1: Introduction and state estimation," *Journal of Power Sources,* vol. 161, no. 2, pp. 1356-1368, 2006.

[4] G. L. Plett, "Sigma-point Kalman filtering for battery management systems of LiPB-based HEV battery packs: Part 2: Simultaneous state and parameter estimation," *Journal of Power Sources,* vol. 161, no. 2, pp. 1369-1384, 2006.

[5] H. Rahimi-Eichi, F. Baronti and M.-Y. Chow, "Online adaptive parameter identification and state-of-charge coestimation for lithium-polymer battery cells," *Industrial Electronics, IEEE Transactions on,* vol. 61, no. 4, pp. 2053-2061, 2014.

[6] W. Waag, C. Fleischer and D. U. Sauer, "On-line estimation of lithium-ion battery impedance parameters using a novel varied-parameters approach," *Journal of Power Sources,* vol. 237, pp. 260-269, 2013.

[7] C. Fleischer, W. Waag, Z. Bai and D. U. Sauer, "On-line self-learning time forward voltage prognosis for lithium-ion batteries using adaptive neuro-fuzzy inference system," *Journal of Power Sources,* vol. 243, no. 1, pp. 728-749, 2013.

[8] S. Wang, M. Verbrugge, J. S. Wang and P. Liu, "Multi-parameter battery state estimator based on the adaptive and direct solution of the governing differential equations," *Journal of Power Sources,* vol. 196, no. 20, pp. 8735-8741, 2011.

[9] R. Xiong, H. He, F. Sun, X. Liu and Z. Liu, "Model-based state of charge and peak power capability joint estimation of lithium-ion battery in plug-in hybrid electric vehicles," *Journal of Power Sources,* vol. 229, pp. 159-169, 2013.

[10] J. Remmlinger, M. Buchholz, M. Meiler, P. Bernreuter and K. Dietmayer, "State-of-health monitoring of lithium-ion batteries in electric vehicles by on-board internal resistance estimation," *Journal of Power Sources,* vol. 196, no. 12, pp. 5357-5363, 2011.

[11] S. Lee, J. Kim, J. Lee and B. H. Cho, "State-of-charge and capacity estimation of lithium-ion battery using a new open-circuit voltage versus state-of-charge," *Journal of Power Sources,* vol. 185, no. 2, pp. 1367-1373, 2008.

[12] Y.-H. Chiang, W.-Y. Sean and J.-C. Ke, "Online estimation of internal resistance and open-circuit voltage of lithium-ion batteries in electric vehicles," *Journal of Power Sources,* vol. 196, no. 8, pp. 3921-3932, 2011.

[13] J. Kowal, D. Schulte, D. U. Sauer and E. Karden, "Simulation of the current distribution in lead-acid batteries to investigate the dynamic charge acceptance in flooded SLI batteries," *Journal of Power Sources,* vol. 191, no. 1, pp. 42-50, 2009.

[14] M. Thele, J. Schiffer, E. Karden, E. Surewaard and D. U. Sauer, "Modeling of the charge acceptance of lead--acid batteries," *Journal of Power Sources,* vol. 168, no. 1, pp. 31-39, 2007.

[15] D. U. Sauer and H. Wenzl, "Comparison of different approaches for lifetime prediction of electrochemical systems—Using lead-acid batteries as example," *Journal of Power Sources,* vol. 176, no. 2, pp. 534-546, 2008.

[16] J. Gou, A. Lee and J. Pyko, "Modeling of the cranking and charging processes of conventional valve regulated lead acid (VRLA) batteries in micro-hybrid applications," *Journal of Power Sources,* vol. 263, pp. 186-194, 2014.

[17] W. Waag, C. Fleischer and D. U. Sauer, "Critical review of the methods for monitoring of lithium-ion batteries in electric and hybrid vehicles," *Journal of Power Sources,* vol. 258, pp. 321-339, 2014.

[18] S. M. Rezvanizaniani, Z. Liu, Y. Chen and J. Lee, "Review and recent advances in battery health monitoring and prognostics technologies for electric vehicle (EV) safety and mobility," *Journal of Power Sources,* vol. 256, pp. 110-124, 2014.

[19] L. Juang, P. J. Kollmeyer, T. M. Jahns and R. D. Lorenz, "System identification-based lead-acid battery online monitoring system for electric vehicles," in *Energy Conversion Congress and Exposition*, 2010.

[20] X. Zhang, R. Grube, K.-K. Shin, M. Salman and R. S. Conell, "Parity-relation-based state-of-health monitoring of lead acid batteries for automotive applications," *Control Engineering Practice,* vol. 19, no. 6, pp. 555-563, 2011.

[21] O. Bohlen, J. Gerschler, D. Sauer, P. Birke and M. Keller, "Robust algorithms for a reliable battery diagnosis-managing batteries in hybrid electric vehicles," in *Proc. The 22nd International Battery, Hybrid and Fuel Cell Electric Vehicle Symposium \& Exposition*, 2006.

[22] C. Fleischer, W. Waag, Z. Bai and D. U. Sauer, "Adaptive On-line State-of-available-power Prediction of Lithium-ion Batteries," *Journal of Power Electronics,* vol. 13, no. 4, pp. 516-527, 2013.

[23] G. L. Plett, "High-performance battery-pack power estimation using a dynamic cell model," *Vehicular Technology, IEEE Transactions on,* vol. 53, no. 5, pp. 1586 - 1593, 2004.

[24] W. Waag, C. Fleischer and D. U. Sauer, "Adaptive on-line prediction of the available power of lithium-ion batteries," *Journal of Power Sources,* vol. 242, pp. 548-559, 2013.

[25] K. S. Champlin and K. Bertness, "Results of discrete frequency immittance spectroscopy (DFIS) measurements of lead acid batteries," in *IEE conference publication*, 2001.

[26] R. Mingant, J. Bernard and V. Sauvant-Moynot, "EIS measurements for determining the SOC and SOH of Li-ion batteries," *The Electrochemical Society,* vol. 33, no. 39, pp. 41-53, 2011.

[27] A. P. Schmidt, M. Bitzer, A. W. Imre and L. Guzzella, "Experiment-driven electrochemical modeling and systematic parameterization for a lithium-ion battery cell," *Journal of Power Sources,* vol. 195, no. 15, p. 5071–5080, 2010.

[28] S. J. Moura, N. A. Chaturvedi and M. Krstic, "Adaptive Partial Differential Equation Observer for Battery State-of-Charge/State-of-Health Estimation Via an Electrochemical Model," *Journal of Dynamic Systems, Measurement, and Control,* vol. 136, no. 1, p. 011015, Oct 2014.

[29] G. K. Prasad and C. D. Rahn, "Model based identification of aging parameters in lithium ion batteries," *Journal of Power Sources,* vol. 232, pp. 79-85, 2013.

[30] M. F. Samadi, S. M. M. Alavi and M. Saif, "An electrochemical model-based particle filter approach for Lithium-ion battery estimation," in *Decision and Control (CDC), 2012 IEEE 51st Annual Conference on*, 2012.

[31] P. J. van Bree, A. Veltman, W. H. A. Hendrix and P. P. J. van den Bosch, "Prediction of battery behavior subject to high-rate partial state of charge," *Vehicular Technology, IEEE Transactions on,* vol. 58, no. 2, pp. 588-595, 2009.

[32] X. Wei, . X. Zhao and Y. Yuan, "Study of equivalent circuit model for lead-acid batteries in electric vehicle," in *Measuring Technology and Mechatronics Automation, 2009. ICMTMA'09. International Conference on*, 2009.

[33] F. Huet, "A review of impedance measurements for determination of the state-of-charge or state-of-health of secondary batteries," *Journal of Power Sources,* vol. 70, no. 1, pp. 59-69, 1998.

[34] P. Singh and D. Reisner, "Fuzzy logic-based state-of-health determination of lead acid batteries," in *Telecommunications Energy Conference*, 2002.

[35] P. E. Pascoe, H. Sirisena and A. H. Anbuky, "Coup de fouet based VRLA battery capacity estimation," in *IEEE International Workshop on Electronic Design, Test and Applications*, 2002.

[36] H. Rahimi-Eichi and M.-Y. Chow , "Adaptive online battery parameters/SOC/capacity co-estimation," in *Transportation Electrification Conference and Expo (ITEC)*, 2013.

[37] G. L. Plett, "Recursive approximate weighted total least squares estimation of battery cell total capacity," *Journal of Power Sources,* vol. 196, no. 4, p. 2319–2331, 2011.

[38] B. S. Bhangu, P. Bentley, D. A. Stone and C. M. Bingham, "Nonlinear observers for predicting state-of-charge and state-of-health of lead-acid batteries for hybrid-electric vehicles," *IEEE Transactions on Vehicular Technology,* vol. 54, no. 3, pp. 783-794, 2005.

[39] B. Bhangu, P. Bentley, D. A. Stone and C. M. Bingham, "State-of-charge and state-of-health prediction of lead-acid batteries for hybrid electric vehicles using non-linear observers," *Institute of Electronic and Electrical Engineering,* 2005.

[40] M. Barak, Electrochemical power sources: primary and secondary batteries, London & New York: IET, 1980.

Appendix

Aging Mechanisms

Aging Mechanisms	Characteristics	Causes	Solution
Anodic corrosion / Side reactions	Grid corrosion at positive plates	Over-charging	Unavoidable but slow
	Corrosion at negative plates	Acid depletion due to water loss	Maintain in high SOC
Positive active material degradation	Loss of contact between individual particles of the positive active material and grid	1. Cycling 2. Deep discharging with high current	1. Charging with high current or high temperature 2. Increase mechanical compression
Crystallization / Sulfation	1. Formation of irreversible crystalline lead sulfate 2. Mainly in negative plates	1. Insufficient charging 2. Long periods of discharge at very low current (self-discharge)	Unavoidable
Short-circuits	Across the separators	High acid concentration	Addition of Na_2SO_4
	Due to positive active material degradation	Same with positive active material degradation	Same with positive active material degradation

Causes and Symptoms of Batteries Failure

Failure modes	Battery type	Causes	Symptoms
Sediment build-up	Flooded	Excessive cycling	Voltage drop
Top lead corrosion	Flooded	Heat generated by large current	Short circuit
Positive grid corrosion	Flooded, VRLA	Oxidation	Increase of internal resistance
Plate sulphation	Flooded, VRLA	Incomplete recharge after over-discharging	Increase of internal resistance and capacity fade
Soft (dendritic) shorts	VRLA	Over-discharging	Decrease of internal resistance and voltage drop
Dry-out and Thermal run-away	VRLA	Lack of proper ventilation, over-charging	Increase of internal resistance and capacity fade